Electrochimica Acta 477 (2024) 143766

Contents lists available at ScienceDirect

Electrochimica Acta

journal homepage: www.journals.elsevier.com/electrochimica-acta

# A critical review of models for density, viscosity, and diffusivity in aqueous sodium chloride solutions

Fazlollah Madani Sani *, Srdjan Nesic

*Institute for Corrosion and Multiphase Technology, Department of Chemical and Biomolecular Engineering, Ohio University, 342 West State St., Athens, OH, 45701, USA*

ARTICLE INFO

*Keywords:*
Solution density
Solution viscosity
Diffusivity
Sodium chloride solutions
Limiting current density

ABSTRACT

Natural brines are extensively produced or used across an array of industries, ranging from oil and gas, geothermal, mining and chemicals to water treatment, desalination, and food industries. Various operational challenges arise when working with these brines, such as corrosion issues, equipment compatibility, or process optimization, highlighting the need for accurate estimation of their key physical properties, specifically density, viscosity, and diffusivity. The direct measurement of these properties often proves to be a formidable task, promoting the adoption of the estimation models as a practical solution. These predictive models find their relevance in a wide spectrum of domains, including corrosion analysis, carbon capture endeavors, geothermal energy recovery, critical mineral mining, desalination, and water treatment. The present review critically evaluates widely cited and publicly available models for density, viscosity, and diffusivity of dissolved species in brines. The performance of these models is assessed based on their validity range, accuracy, and ease of implementation by comparing them with experimental data from literature as a benchmark. Furthermore, the values for diffusivity of multiple species at 25°C and infinite dilution in water are reevaluated. For more accurate estimation of diffusivity at various temperatures and salt concentrations, new coefficients are introduced for selected species. As an illustrative example, the contribution of these three properties to the prediction of electrochemical limiting current density, a crucial parameter with applications in diverse research and industrial fields, is systematically analyzed by comparing calculated values with measurements in aqueous NaCl solutions. The results indicate that accuracy of estimating diffusivity in brines outweighs the significance of estimating solution density and viscosity in limiting current density calculations.

## 1. Introduction

Natural brines can be produced or utilized in diverse processes across industries such as oil and gas [1–4], geothermal [5,6], mining [7,8], chemicals [9,10], water treatment and desalination [11,12], as well as food processing [13–15]. To take one example, in the oil and gas sector, brines (known as produced waters) are generally recovered during hydrocarbon extraction from both conventional and unconventional oil and gas wells. There are reports that on average for every barrel of crude oil extracted from conventional oil reservoirs, between 7 to 10 barrels of brine are produced [1,16–19]. This amount is usually lower for gas reservoirs. The amount of produced water in primary production increases over time when reservoirs deplete and this amount can be even higher if secondary or tertiary recovery methods are used, reaching as high as 100 barrels of brine for every barrel of oil [19,20]. In the United States, for instance, around 2.5 billion gallons of produced water was extracted alongside oil and gas every day in 2018 [20]. In another example – the geothermal industry, depending on the geothermal resource characteristics, efficiency of the power plant, and the design of the geothermal system, on average between 200 to 1000 gallons of brine per hour is required to generate 1 megawatt of electricity [21–23].

Dealing with natural brines introduces a range of operational challenges such as corrosion issues, equipment compatibility, process efficiency and optimization, environmental concerns, *etc.* in various industries. Taking the two previously mentioned examples into account, the oil and gas industry faces a continuous concern with corrosion damages to metallic parts and equipment exposed to brines [24,25]. To effectively address this concern, corrosion rate prediction models serve as essential tools for producers and operators, enabling them to select suitable materials, optimize operational conditions, and implement timely and effective corrosion mitigation strategies. In order to develop accurate corrosion rate prediction models suitable for natural brine

* Corresponding author.
*E-mail address:* fm874012@ohio.edu (F. Madani Sani).

https://doi.org/10.1016/j.electacta.2024.143766
Received 3 November 2023; Received in revised form 22 December 2023; Accepted 2 January 2024
Available online 4 January 2024

**Table 1**
The evaluated density models for aqueous NaCl solutions and their range of validity.

| Density model | Validity range | | |
|---|---|---|---|
| | Temperature (°C) | Pressure (bar) | NaCl concentration |
| Novotny and Sohnel [45,46] | 0–100 | N/A | 0-saturation |
| Batzle and Wang [41] | 0–350 | 1–981 | 0–5.4 m (0–24 wt.%) |
| Rogers and Pitzer [43] | 0–300 | 1–1000 | 0–5 m (0-22.6 wt.%) |
| Driesner [51] | 0–1000 | 1–5000 | 0–1 $X_{NaCl}$ |
| Mao and Duan [52] | 0–300 | 1–1000 | 0–6 m (0–26 wt.%) |

m is molality, wt.% is salt weight percent, and $X_{NaCl}$ is NaCl mole fraction.

environments, it is essential to determine key physical properties of the brines, naming solution density, solution viscosity, and diffusivity of dissolved species. Furthermore, these properties hold equal significance in the geothermal industry. The density of brine affects its buoyancy, which in turn influences its circulation within geothermal reservoirs. Viscosity directly impacts heat transfer efficiency within geothermal systems and diffusivity of dissolved species influences the distribution of heat, minerals, and other components in the geothermal reservoir.

Measuring solution density, solution viscosity, and diffusivity of dissolved species accurately can be challenging and impractical and often it is found that their in-situ values differ from those measured at sampling ports or in laboratory settings. An alternative approach that is fast, easy, and cost-effective is to use models to calculate these parameters under the specific operational conditions of interest. The main challenge lies in finding accurate, yet straightforward models that can cover a wide range of operational conditions, such as temperature, pressure, and chemical composition, ensuring their applicability in real-world scenarios. When addressing corrosion issues, this very challenge appears to be the reason why the majority of aqueous corrosion models found in the open literature or even available commercially are based on models developed specifically for pure water or very dilute salt solutions, as there are more experimental data and models available for these systems compared to the concentrated brines [26–31]. However, it is important to note that brines typically have salinity levels exceeding 3 wt.% [19,32–34]. For example, half of the conventional oil wells in the USA produce brines containing more than 10 wt.% salt [35]. Therefore, using suitable models to estimate the physical properties of brines is crucial for ensuring the reliability of corrosion modeling efforts.

The following text provides a critical review and comparison of publicly available models that describe density and viscosity of concentrated aqueous salt solutions as well as diffusivity of dissolved species in such solutions. The objective was to identify the most suitable models based on their range of validity, accuracy, and ease of implementation for each physical property. To validate these models, they were combined and tested by comparing them against electrochemical measurements in aqueous solutions. However, the models discussed in this article are applicable beyond aqueous corrosion modeling in the oil and gas industry. They can be effectively utilized in various fields such as carbon capture, utilization and storage, geothermal energy recovery, lithium and other critical mineral mining, as well as desalination and water treatment.

It is important to note that the models presented below are specifically tailored for aqueous NaCl solutions, given that NaCl is the predominant dissolved salt in natural brines [32,36–38]. For example, on average, about 80 % of total dissolved solids in produced water and geothermal brines is NaCl [35,39]. However, a similar approach can be employed to extend the applicability of the models to encompass other commonly found salts such as calcium chloride, magnesium chloride, and magnesium sulfate.

## 2. Review and validation of models for density of aqueous NaCl solutions

When salt, such as NaCl, is added to water, the salt crystal dissolves in water as a result of stronger interactions (forces) between ions and water molecules (solvent) compared to the interionic forces within the salt crystal [40]. The resulting dissociated ions become surrounded by water molecules. This phenomenon is termed hydration or, more broadly, solvation. The mass of solution increases to a greater degree than its volume due to the higher density of salt relative to water. As a result, the solution density increases with a rise in salt concentration. There are several models in the literature for calculating the density of aqueous NaCl solutions [41–52]. Some of these models are empirical in nature [41,42,45–47], while others are semi-empirical [43,44,48–52]. In some cases, the calculation of pure water density is a prerequisite for determining salt solution density, necessitating a separate model [43,44,47–49,51]. Multiple models are available in the literature for calculating density of pure water [53–55,41,56–58].

In the following review, five well-recognized density models for aqueous NaCl solutions are compared against each other and experimental data in order to assess their performance. The name of these models and their validity range are listed in Table 1. The first two models are purely empirical using simple equations. However, the remaining three models adopt a semi-empirical approach, entailing more intricate calculations. All models except the Novotny and Sohnel [45,46] model express solution density as a function of temperature, pressure, and NaCl concentration, whereas, the Novotny and Sohnel [45,46] density model is just a function of temperature and NaCl concentration. Fig. 1 offers a performance comparison of these models across a range of temperatures, pressures, and NaCl concentrations frequently encountered in practical scenarios. At lower temperatures (Fig. 1a and c), all five models exhibit satisfactory accuracy across the entire spectrum of NaCl concentrations. However, as temperature rises (Fig. 1b, d, and e), the Mao and Duan [52] model begins to overpredict experimental density values for NaCl concentrations exceeding approximately 15 wt.%. A similar trend is observed with the Novotny and Sohnel [45,46] model at temperatures surpassing 100°C (Fig. 1d), as anticipated considering its validation range up to 100°C.

Table 2 provides an overview of each model's performance under different conditions, evaluated in terms of the root-mean-square error (RMSE), with an overall assessment provided. A lower RMSE signifies a higher level of model accuracy. The Rogers and Pitzer [43] model demonstrates the highest accuracy, closely trailed by the Driesner [51] model. The Rogers and Pitzer [43] model has a high degree of complexity, characterized by numerous equations and parameters. Similarly, the Driesner [51] model maintains a comparable level of complexity when adhering to its recommended approach for calculating pure water density—the IAPS-84[1] equation of state [54]. However,

[1] IAPS stands for the International Association for the Properties of Steam, which later changed its name to the International Association for the Properties of Water and Steam (IAPWS).

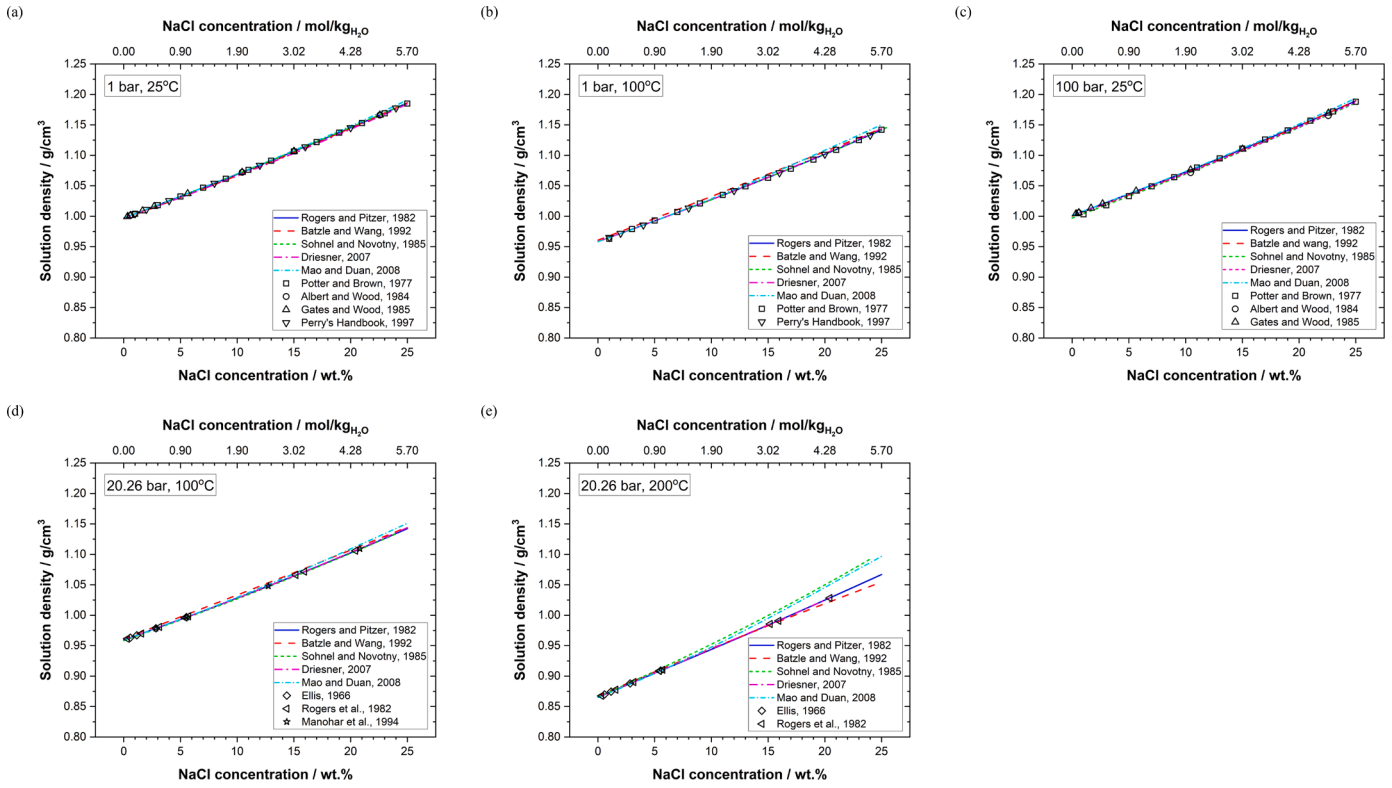


**Fig. 1.** Comparison between calculated (lines) and experimental (dots) density values for aqueous NaCl solutions at (a) 1 bar and 25°C, (b) 1 bar and 100°C, (c) 100 bar and 25°C, (d) 20.26 bar and 100°C, and (e) 20.26 bar and 200°C. Pressures are total pressure. Experimental data are taken from [47,59–64].

**Table 2**
The root-mean-square error (RMSE[2]) × 1000 for the five models at different conditions. N represents the number of experimental data points against which the models were compared.

| Conditions | N | RMSE | | | | |
|---|---|---|---|---|---|---|
| | | Novotny and Sohnel [45,46] | Batzle and Wang [41] | Rogers and Pitzer [43] | Driesner [51] | Mao and Duan [52] |
| 1 bar, 25°C | 32 | 0.43 | 1.55 | 0.24 | 2.10 | 2.10 |
| 1 bar, 100°C | 21 | 0.75 | 4.48 | 0.68 | 1.17 | 4.62 |
| 100 bar, 25°C | 24 | 3.18 | 1.98 | 2.19 | 3.20 | 2.63 |
| 20.26 bar, 100°C | 16 | 1.12 | 3.86 | 0.13 | 0.32 | 2.77 |
| 20.26 bar, 200°C | 12 | 5.50 | 2.59 | 0.31 | 0.44 | 8.07 |
| All conditions | 105 | 2.48 | 2.94 | 1.10 | 1.71 | 4.07 |

simplification is possible by substituting a validated simple pure water density model for the IAPS-84 model, effectively reducing the intricacy of the Driesner [51] model. The Batzle and Wang [41] model shows strong accuracy across the entire tested range. The Batzle and Wang [41] model is a suitable option for various field applications, where accuracy and ease of replication are essential. Comparatively, the Novotny and Sohnel [45,46] model is even simpler than the Batzle and Wang [41] model and remains valid up to 100°C, which is suitable for many practical applications. Another advantage of the Novotny and Sohnel [45,46] model is its applicability to over 300 inorganic salt solutions. Particularly for situations involving temperatures below 100°C, which is the norm in most aqueous scenarios, the Novotny and Sohnel [45,46] model proves to be a reliable and effective choice for calculating NaCl solution density.

Examining NaCl solution density across different pressures in Fig. 1, it becomes evident that pressure exerts a negligible impact on solution density. This is easily understandable due to water's near-incompressible nature, preventing pressure from altering the solution volume and consequently its density.

## 3. Review and validation of models for viscosity of aqueous NaCl solutions

Viscosity is a key factor in how fluids flow, and its variations can have a significant effect on the flow regimes. Furthermore, fluid viscosity is related to the diffusivity of dissolved species in the fluid [65]. This point will be discussed in some more details further below. The viscosity of Newtonian fluids like water and aqueous solutions is a strong function of temperature and to a lesser extent, total pressure. It is also affected by the presence of dissolved species such as salts and gases. In corrosion modeling, since both the flow regime (which primarily depends on the Reynolds number), and the mass transfer rates (which depends on both the Reynolds number and the Schmidt number) affect the rate of corrosion, calculating viscosity as a function of temperature and aqueous solution composition needs to be addressed carefully. In the geothermal industry, viscosity directly affects how efficiently heat is

[2] RMSE=$\sqrt{\sum_{i=1}^{n}(p_i - m_i)^2/n}$, where $n$ is total number of observations, $p_i$ is the calculated value and $m_i$ is the measured value for observation $i$.

transferred within geothermal systems. A higher viscosity can impede fluid movement and subsequently hinder the transfer of heat from the reservoir to the surface. In carbon capture and storage (CCS), the brine viscosity affects how easily $CO_2$ can displace the brine during injection into the subsurface, influencing the efficiency of the injection process. Additionally, the viscosity of the brine can influence the sweep efficiency, which is the extent to which the injected $CO_2$ displaces resident brine and occupies available pore spaces. Viscosity also influences the speed and extent of fluid movement, which can impact how and where potential leaks might occur within $CO_2$ storage formations.

The effect of temperature on pure water viscosity is well understood and accurately described by various models [66–71], and this will not be a focal point in the present review. Instead, the focus will be on models that capture the effect of dissolved species, primarily NaCl salt, on the viscosity of aqueous solutions. In the mid-19$^{th}$ century, Poiseuille [72] pioneered research on the effect of salt on water viscosity. Since then, extensive research has been dedicated to this subject. Detailed historical reviews can be found elsewhere [73,74]. Generally, when a salt, such as NaCl, is added to an aqueous solution, the solution viscosity increases, although there are some exceptions. The change in solution viscosity with salt concertation can be explained by looking at the molecular origin of viscosity.

Due to the polar nature of water molecules and the resulting bonds (called hydrogen bonding) between the negative end of one water dipole and the positive end of the other, water molecules form a three-dimensional tetrahedral structure, with each oxygen atom in the water molecule being surrounded by another four oxygen atoms with hydrogen atoms in between. Hydrogen bonding creates a network of interconnected molecules that resist shear deformation imposed by flow. This resistance on a macroscopic level can be described by the concept of viscosity. When a salt, for example NaCl, is dissolved in liquid water, it is fully dissociated due to the interaction with the surrounding water dipoles. The water dipoles in the immediate vicinity of the dissociated ions are held tightly and are oriented in the electrical field created by the ions. Between these oriented water dipoles and those farther away in the bulk water, a group of water dipoles exists that is neither organized according to the spherical electrical field imposed by the central ion, nor can take up the usual tetrahedral arrangement favored by bulk water dipoles. Overall, the molecular structure of water is changed in the presence of salt ions, consequently affecting the resistance to flow and, by extension, the viscosity of the solution.

When considering the impact of temperature on viscosity, the structure of water molecules, created through hydrogen bonding between water dipoles and electrostatic ion-dipole forces, faces a consistent challenge from the ongoing random thermal motion of water molecules. As temperature increases, the more energetic thermal motion weakens the water structure, resulting in a lower viscosity.

The presence of dissolved salts, can alter the viscosity of solutions in either direction [75], depending on how the introduction of ions affects the structure of water molecules. This phenomenon is best seen in dilute solutions of alkali halide salts. For example, solutions of potassium fluoride (KF) in water are more viscous than pure water, while solutions of potassium iodide (KI) in water are less viscous than pure water. The smaller $F^-$ ion, which has a high hydration number, strengthens the overall structure of water, whereas the larger $I^-$ ion with a low hydration number, weakens the structure. Therefore, ions such as $F^-$ are called 'structure making' ions or *osmotropes,* and ions such as $I^-$ are called 'structure breaking' ions or *chaotropes* [75,76]. The situation can become even more complicated as there are a few salts such as the abovementioned KI but also KCl and CsCl that exhibit both behaviors and can cause the solution viscosity to initially decrease (in dilute solutions) and then increase with rising salt concentration, at low temperatures [77–81]. More on how the variation in concentration of different ions influences the solution viscosity can be found in a paper published by Kwak *et al.* [81]. For the case of NaCl which is the focus of this study, the solution viscosity monotonically increases as the concentration of NaCl increases.

The viscosity of dilute salt solutions is often modeled by the well-known Jones-Dole equation [74] as follows:

$$\frac{\eta_s}{\eta_w} = 1 + A\sqrt{c} + Bc \tag{1}$$

where $\eta_w$ and $\eta_s$ are the viscosities of pure water and salt solution, respectively, $c$ is the molar concentration of solute (salt), and $A$ and $B$ are constants specific to the solute. The second term on the right-hand side of Eq. (1) is called the electrostatic term and is due to long-range Coulombic ion-ion interactions, which tend to provide additional structure to the electrolyte solution. Hence, constant $A$ is zero for non-electrolyte solutions and positive for electrolyte solutions. This electrostatic term can often be neglected at moderate and high concentrations of electrolytes, when it is overwhelmed by the third term, which is called the structural effect and is a measure of ion-water interactions [81]. Constant $A$ can be calculated by an expression proposed by Falkenhagen and Dole [82,83], while $B$ is a solute dependent empirical constant. The basic Jones-Dole Eq. (1) is only valid for relatively dilute solutions, *i.e.*, concentrations not more than 0.2–0.3 M [74,84,85]. For applications at higher concentrations, extended versions of the Jones-Dole equation have been proposed by Kaminsky and others [84–87].

Alternate models have been developed to compute solution viscosity, extending their applicability to a broader range of NaCl concentrations [41,65,84,87–92]. From these, the three highly cited models: the Batzle and Wang [41], the Kestin *et al.* [89,90], and the Mao and Duan [65] models have been reproduced here and compared against experimental data, to identify the most reliable one. The Batzle and Wang [41] model is a simple empirical model, while the Kestin *et al.* [89,90] model is a complex semi-empirical model. The Mao and Duan [65] model is an extended version of the Jones-Dole [77] equation. Table 3 outlines the ranges within which these three models are valid.

Fig. 2 shows the comparison between the three models at five different experimental conditions, selected from the open literature. This comparison aims to evaluate the accuracy of the models across a broad range of temperatures, pressures, and NaCl concentrations frequently encountered in practical scenarios. The original Jones-Dole equation [74] is not included in the comparison, as in its original form was not meant to cover the extensive range of conditions tested in this study. Obviously, all three models capture the general trend correctly – an increase in solution viscosity with increasing NaCl concentration. The Batzle and Wang [41] model does not result in accurate viscosity predictions particularly in the middle range of NaCl concentrations and relatively high temperatures. On the other hand, the Kestin *et al.* [89,90] and the Mao and Duan [65] models predict viscosity values accurately and almost identically for all five tested conditions. Yet, the Mao and Duan [65] model proves to be more practical than the Kestin *et al.* [89, 90] model due to its simplicity in replication and, more importantly, its broader coverage of operational conditions.

Comparing Fig. 2a with Fig. 2c, and likewise, Fig. 2b with Fig. 2d, indicates that the effect of pressure on viscosity of aqueous NaCl solution is negligible, as anticipated. For temperatures below 100°C and NaCl concentrations up to the point of saturation, the changes in viscosity with increasing pressure from 1 bar to 100 bar is less than 0.5 % [41,84, 95]. However, an indirect effect of pressure on brine viscosity arises in

**Table 3**
Viscosity models examined for aqueous NaCl solutions and their applicable validity ranges. m is molality and wt.% denotes salt weight percent.

| Model | Temperature (°C) | Pressure (bar) | NaCl concentration |
|---|---|---|---|
| Batzle and Wang [41] | 0–350 | 1–981 | 0-5.4 m (0–24 wt.%) |
| Kestin *et al.* [89,90] | 20–150 | 1–350 | 0-5.4 m (0–24 wt.%) |
| Mao and Duan [65] | 0–400 | 1–1000 | 0–6.0 m (0–26 wt.%) |

m is molality and wt.% denotes salt weight percent.

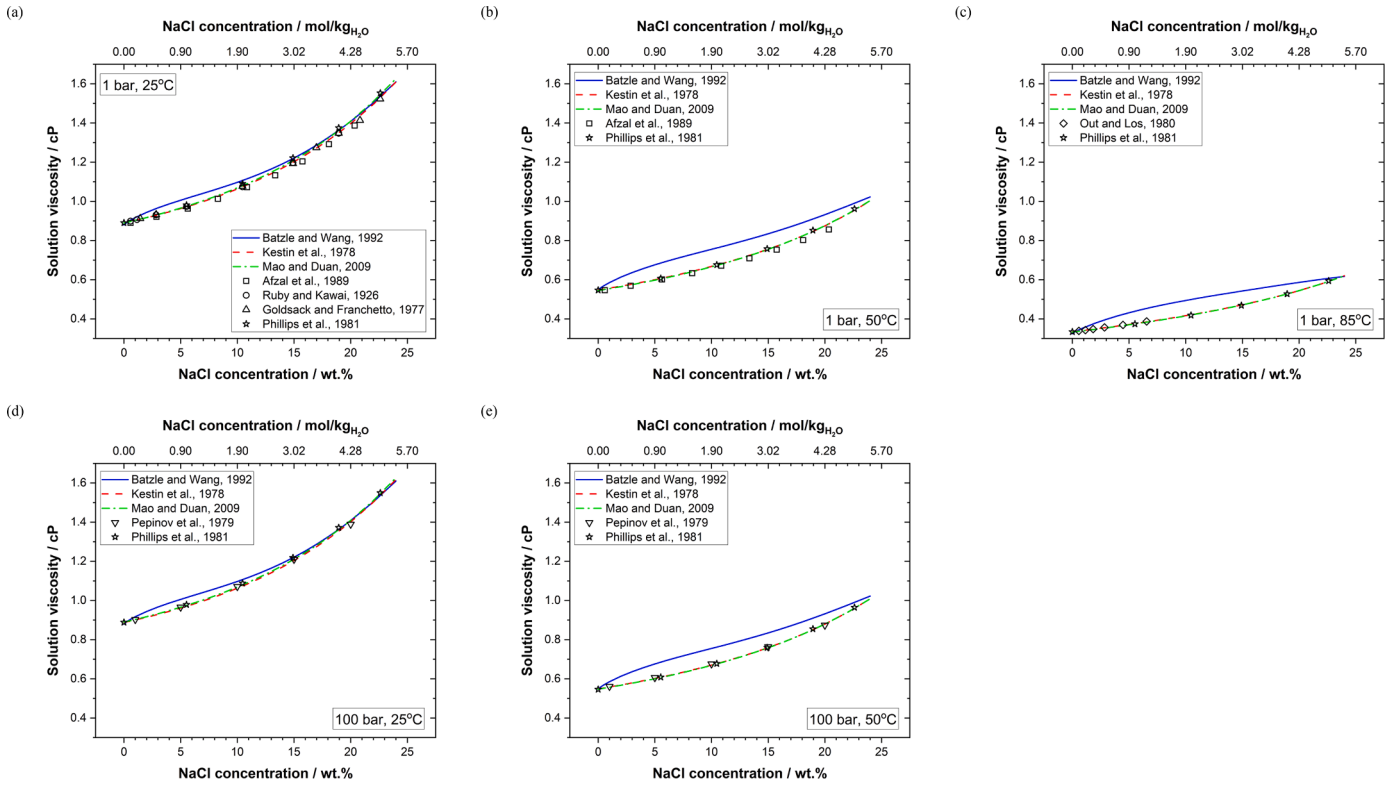


**Fig. 2.** Comparison of three viscosity models [41,65,89,90] for aqueous NaCl solutions. Dynamic viscosities at (a) 1 bar and 25°C, (b) 1 bar and 50°C, (c) 1 bar and 85°C, (d) 100 bar and 25°C, and (e) 100 bar and 50°C. Pressures represent total pressure. Points are experimental data obtained from [79,88,93–96], while solid lines are calculated viscosities.

situations where high partial pressures of acid gases such as $CO_2$ and $H_2S$ exist. This phenomenon is frequently observed in domains such as oil and gas production, geothermal applications, or CCS. The solubility of these gases in aqueous solution increases at higher partial pressures, resulting in a noticeable increase in the solution viscosity.

For example, in the context of corrosion models developed to date for aqueous corrosion of mild steel piping systems and equipment, when acid gases are dissolved in aqueous solutions, the solution viscosity is assumed to remain unchanged and identical to that of an aqueous solution without any dissolved gases [26,97–100]. This assumption might be true at low partial pressures of acid gases (*e.g.*, up to 10 bar) when solubility of gases in the solution is relatively small. However, at high partial pressures, neglecting the presence of dissolved gases in the solution could lead to a substantial margin of error in viscosity predictions, and thereby, mass transfer and corrosion rate calculations. In practical applications within the oil and gas industry, $CO_2$ partial pressure can be very high. For instance, consider wellbores in conventional oil and gas wells, where $CO_2$ partial pressure might surpass 100 bar. Similarly, in $CO_2$ gathering systems, this pressure can peak at around 30 bar. In more advance applications like $CO_2$-enhanced oil recovery ($CO_2$-EOR), the $CO_2$ partial pressure within $CO_2$ transportation lines can be as high as 200 bar, with further increases as approaching the bottom of the injection well [101,102]. Given these circumstances, it becomes prudent to incorporate the influence of acid gas partial pressures into viscosity models, particularly those pertinent to $CO_2$.

To that effect, the Islam and Carlson [92] stands as an extended version of Mao and Duan [65] model, designed to predict the viscosity of aqueous NaCl solutions in the presence of dissolved $CO_2$. Compared to the Mao and Duan [65] model, a simpler equation is used for calculating the density of water in the Islam and Carlson [92] model, instead of the IAPWS 1997 [57] equation used in the Mao and Duan model [65]. To factor the effect of $CO_2$ on NaCl solution viscosity, Islam and Carlson [92] correlated the viscosity of $CO_2$-saturated aqueous NaCl solutions with those containing no $CO_2$. They suggested a correlation that is a function of mole fraction of dissolved $CO_2$ in the solution. However, comparing with the experimental data reported by Bando *et al.* [103] and Fleury and Deschamps [104], it is found that Islam and Carlson [92] equation[3] lacks a temperature dependency. To address this issue, a modification is proposed here for the Islam and Carlson [92] equation as follows:

$$\mu_{sol} = \mu_b \left(1 + 4.65\, x_{CO_2}^{0.0144T - 3.3964}\right) \tag{2}$$

where, $\mu_b$ is viscosity of solution for the $H_2O$-NaCl system, $\mu_{sol}$ is viscosity of solution for the $H_2O$-NaCl-$CO_2$ system, $T$ is the solution temperature in K, and $x_{CO_2}$ is the mole fraction of dissolved $CO_2$ in the solution. It is assumed that the concentration of other species in the solution produced due to $CO_2$ dissociation is negligible compared to the concentration of dissolved $CO_2$. The average absolute deviation[4] from the Bando *et al.* [103] experimental data for the newly proposed Eq. (2) amounts to 1.18 %, lower than the 3.39 % derived from the original Islam and Carlson [92] equation. When compared with the Fleury and Deschamps [104] experimental data, the viscosity values calculated by the new equation shows an average deviation of 3.62 %, outperforming the 4.10 % deviation obtained by the original Islam and Carlson [92] equation.

Therefore, an extension of the Islam and Carlson [92] to include the

[3] The Islam and Carlson's [92] equation is presented as a function of the dissolved $CO_2$ mole fraction in their article. However, the calculated viscosity values plotted in Fig. 7 of their article are reproducible when the mass fraction of dissolved $CO_2$ is used instead of the mole fraction. This contradiction appears to be incorrect and misleading.

[4] Absolute deviation$= \frac{|\mu_{exp} - \mu_{cal}|}{\mu_{exp}} \times 100$, where $\mu_{exp}$ is measured viscosity and $\mu_{cal}$ is calculated viscosity.

effect of dissolved $CO_2$ via Eq. (2) is suggested as the recommended approach for calculating the viscosity of aqueous NaCl solutions saturated with $CO_2$ gas. The validity range of the Mao and Duan [65] model is 1°C < T < 350°C, 1 bar < P < 1000 bar, and 0 m < NaCl < 6 m and Eq. (2) is expected to be valid for conditions up to 100°C, $CO_2$ partial pressure of 100 bar, and NaCl concentration of 6 m.

To assess the performance of the extended model, the effect of total pressure and dissolution of $CO_2$ gas on viscosity of aqueous NaCl solution is shown at 30°C and varying NaCl concentrations in Fig. 3. The solid lines represent solution viscosity values obtained with the extended model, Eq (2). Meanwhile, the dashed and dotted lines correspond to solution viscosity values calculated using the Mao and Duan [65] model. For $CO_2$ saturated NaCl solutions at 30°C, only a few experimental data points could be found in the literature. These data points have been compared with the calculated viscosity values in Fig. 3. In the absence of $CO_2$, the viscosity of NaCl solution is virtually the same at all three total pressures over the entire NaCl concentration range. This confirms that pressure has a minimal impact on solution viscosity [41,84,95]. However, in the presence of $CO_2$, the viscosity of NaCl solution is higher owing to $CO_2$ dissolution. This rise in solution viscosity becomes more pronounced with higher $CO_2$ partial pressures. For example, in pure water (0 wt.% NaCl), the introduction of $CO_2$ at 100 bar increases solution viscosity by around 12 %. At higher NaCl concentrations, the viscosity gap between the $CO_2$-saturated solutions and those without $CO_2$ becomes smaller due to salting out of $CO_2$, which has been explained elsewhere [105,106].

When considering the presence of other gases in operational scenarios, it is reasonable to expect that the increase in solution viscosity due to their dissolution would follow a similar pattern to what is observed with $CO_2$, once differences in solubilities are factored in. As an example, take $H_2S$ gas, a common gas in the oil and gas and geothermal fields. $H_2S$ dissolves in aqueous NaCl solutions approximately three times higher than $CO_2$. However, the typical partial pressures of $H_2S$ seen in real field conditions are generally much lower in comparison to $CO_2$, resulting in a proportionally smaller quantity of dissolved $H_2S$ in the solution. Therefore, in many cases the effect of dissolved $H_2S$ on viscosity of the aqueous solutions can be disregarded for the purpose of modeling.

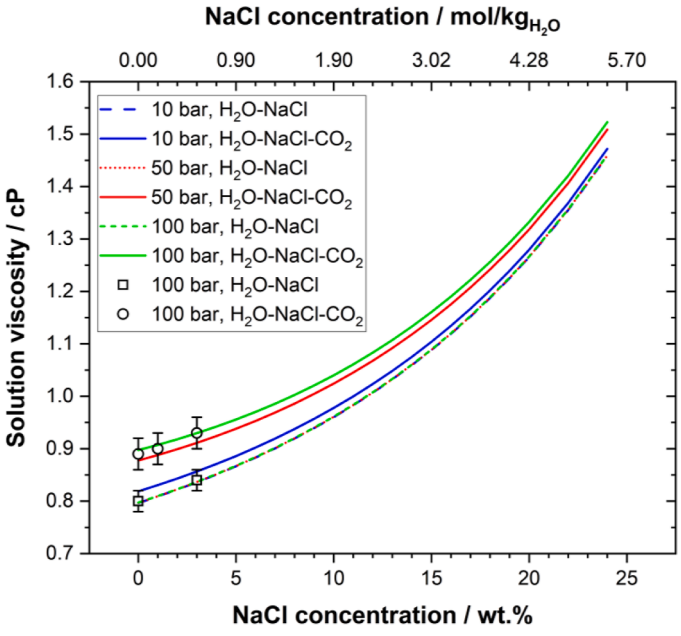


**Fig. 3.** The effect of pressure and dissolved $CO_2$ on dynamic viscosity of NaCl aqueous solutions in an open system at 30°C. The solid lines are calculated with a modified version of the Islam and Carlson model [92], Eq. (2). The dashed and the dotted lines are obtained with the Mao and Duan [65] model. The experimental data points are taken from [103].

## 4. Review and validation of models for diffusivity of dissolved species in aqueous NaCl solutions

Diffusivity, also referred to as diffusion coefficient, of dissolved species in aqueous electrolyte solutions holds immense significance for calculating mass transfer rates in a wide array of applications such as distillation, desalination, membrane and chemical separation process, mixing process, hydrometallurgy, adsorption, coatings, geothermal reservoir fluid-rock interaction, drug delivery, environmental monitoring and remediation, batteries, fuel cells, electrochemical devices and sensors, and corrosion modeling. In many of the processes mentioned above, particularly those involving heterogeneous reactions, diffusion of aqueous species can be a determining factor for the rate of the process [107]. Hence, precise insights into diffusivity behavior under varying conditions is essential for accurately gauging the rate of such process [108,109].

Obtaining diffusivity values can be achieved through two main approaches: direct measurements and the utilization of diffusivity models. Diffusivity measurements are inherently laborious, time-consuming, and expensive. The complexity of measurements escalates when multiple dissolved species are present in the solution [110,111]. As such, utilizing estimation models offers an appealing alternative to direct diffusivity measurement. However, it is important to recognize that most of these estimation models necessitate experimental data to calibrate their coefficients and constants.

Various techniques are available for measuring diffusivity of aqueous species (ions, neutral, soluble gases) [112,113]. Some of these techniques, the data of which is also used in this review, are: diaphragm cell [114–119], stagnant diffusion cell [120–123], Gouy interferometric [112,124], microfluidic channel [125,126], absorption onto wetted wall-column [127–129] and sphere [130–132], absorption into laminar [133–143] and annular [144] jets, absorption into a thin film [139,145], diffusion in laminar flow in pipe [146–149], capillary electrophoresis [143], mercury polarography [150–155], polarographic electrode [156,157], liquid droplet dissolution [158], collapse of stationary bubble [159–162], spectrophotometric [163,164], electrical resistivity [165,166], chronoamperometry [167], electrochemical limiting diffusion current [168], and pulse-field gradient nuclear magnetic resonance (PFG-NMR) [169]. It is essential to note that each of these techniques carries inherent measurement errors [135,144,145,170,171] that must be considered when utilized for model calibration. Among these methods, PFG-NMR stands out as a relatively new approach for measuring self-diffusion in aqueous solutions [172,173]. PFG-NMR offers rapid measurements, demands minimal preparation, and utilizes small sample volumes. Importantly, its application does not significantly perturb the studied system. Unlike the isotopic tracer method, which is influenced by interfering isotope effects, PFG-NMR measures the "true" diffusivity. Additionally, PFG-NMR allows for the measurement of both neutral and charged species in aqueous solutions across a wide range of temperatures, pressures, and concentrations [171,174,175].

Calibrating models becomes particularly challenging when only limited data is available for a specific species. Nevertheless, the process of estimating diffusivity typically follows a two-step protocol: (1) determining the effect of pressure and temperature on diffusivity, (2) accounting for the effect of salt concentration on diffusivity. This has been demonstrated in detail below.

Broadly, two distinctive types of diffusion processes can be identified: (1) self-diffusion, also called tracer diffusion, single-ion diffusion, ionic diffusion, and (2) mutual diffusion, also referred to as interdiffusion, concentration diffusion, salt diffusion. Self-diffusion is associated with the random motion of individual species in a solution, where each species has an equal opportunity to occupy any point within the total space occupied by the solvent [176–178]. This form of diffusion carries particular importance in processes involving aqueous electrolyte

solutions and is the primary focus of this review. Hereafter, within the text, the terms "diffusion" and "diffusivity" refer to self-diffusion.

The temperature and concentration dependencies of diffusivity can be explored by considering the diffusion flux density ($N_i$) as a function of the gradient of chemical potential:

$$N_i = -u_i c_i^{'} \nabla \mu_i \tag{3}$$

where, $N_i$ in mol/cm$^2$/s is a vector quantity that indicates the direction in which dissolved species $i$ is diffusing in the solution with the magnitude representing the number of moles of species $i$ passing across a plane of 1 cm$^2$ normal to the diffusion direction per second, $u_i$ is the mobility of dissolved species $i$ in cm$^2$·mol/J/s and represents the average velocity of that species in the solution when a force of 1 N/mol is applied to the species, $c_i^{'}$ is concentration of dissolved species $i$ in mol/cm$^3$, and $\mu_i$ is the chemical potential[5] of dissolved species $i$ in J/mol. The gradient ($\nabla$) of chemical potential ($\nabla\mu_i$) serves as the driving force for the mass transfer. For a uniform mass transfer across the surface, the gradient of chemical potential can be assumed to be non-zero in the direction perpendicular to the surface ($x$), while being zero in the other two directions. This assumption finds applicability in various processes such as electroplating, electrolysis, battery charge and discharge cycles, electrochemistry, corrosion, *etc*. Thus, for a one-dimensional domain in the $x$ direction, perpendicular to the surface, Eq. (3) can be simplified as follows:

$$N_i = -u_i c_i^{'} \frac{d\mu_i}{dx} \tag{4}$$

The thermodynamic definition of chemical potential can be presented in the subsequent manner:

$$\mu_i = \mu_i^0 + RTln\left(\gamma_i^c c_i\right) \tag{5}$$

where $\mu_i^0$ is the standard chemical potential of species $i$ at a given temperature in J/mol in the molarity concentration unit system, $R$ is the universal gas constant in J/mol/K, $T$ is temperature in K, $c_i$ is concentration of species $i$ in molarity (M), $\gamma_i^c$ is the molarity-based activity coefficient of species $i$, and $x$ represents the distance of species $i$ from the surface in cm. Substituting this definition into Eq. (4) yields [40]:

$$\begin{aligned}
N_i &= -u_i c_i^{'} \frac{d}{dx}\left(\mu_i^o + RTln\left(\gamma_i^c c_i\right)\right) \\
&= -\frac{u_i c_i}{1000}\frac{d}{dx}\left(\mu_i^o + RTln\left(\gamma_i^c c_i\right)\right) \\
&= -\frac{u_i c_i}{1000}\frac{RT}{\gamma_i^c c_i}\frac{d}{dx}\left(\gamma_i^c c_i\right) \\
&= -\frac{u_i}{1000}\frac{RT}{\gamma_i^c}\left(\gamma_i^c\frac{dc_i}{dx} + c_i\frac{d\gamma_i^c}{dx}\right) \\
&= -\frac{u_i RT}{1000}\frac{dc_i}{dx} - \frac{u_i RT c_i}{1000\gamma_i^c}\frac{d\gamma_i^c}{dx} \\
&= -\frac{u_i RT}{1000}\frac{dc_i}{dx} - \frac{u_i RT c_i}{1000\gamma_i^c}\frac{d\gamma_i^c}{dc_i}\frac{dc_i}{dx} \\
&= -\frac{u_i RT}{1000}\frac{dc_i}{dx}\left(1 + \frac{c_i}{\gamma_i^c}\frac{d\gamma_i^c}{dc_i}\right) \\
&= -\frac{u_i RT}{1000}\frac{dc_i}{dx}\left(1 + \frac{dln\gamma_i^c}{dlnc_i}\right)
\end{aligned} \tag{6}$$

Finally, recalling the Fick's first law of diffusion [40]:

$$N_i = -D_i\frac{dc_i^{'}}{dx} \tag{7}$$

where $D_i$ is diffusivity or diffusion coefficient of species $i$ in cm$^2$/s. Expressing Eq. (7) in molarity concentration unit gives:[6]

$$N_i = -\frac{D_i}{1000}\frac{dc_i}{dx} \tag{8}$$

By equating Eqs. (6) and (8), we obtain an expression for diffusivity:

$$D_i = u_i RT\left(1 + \frac{dln\gamma_i^c}{dlnc_i}\right) \tag{9}$$

Eq. (9) implies that, at a constant temperature, $D_i$ depends on the mobility ($u_i$) and activity coefficient ($\gamma_i^c$) of species $i$. Since $\gamma_i^c$ is a function of concentrations of all the species in the solution [179,180], $D_i$ consequently relies on the concentrations of all those species as well. However, in situations where species $i$ is present in trace concentrations within a strong electrolyte (salt) solution, such as NaCl, *i.e.*, when $c_i$ is much smaller than the concentration of dissociated salt ions (in this case $c_{Na^+}$ and $c_{Cl^-}$), it follows that $\gamma_i^c$ depends only on the concentration of salt ions alone. If the dissociated salt ions are not electroactive (*i.e.*, they are not consumed or produced throughout the process) and their concentrations are uniform across the mass transfer domain, the concentration-dependent term in Eq. (9), $dln\gamma_i^c/dlnc_i$ approximates zero. As a result, the diffusivity expression simplifies to [40,181]:

$$D_i = u_i RT \tag{10}$$

Eq. (10) suggests that for strong electrolyte (salt) solutions, diffusivity of any electroactive species is solely dependent on two factors: species' mobility in the solution, which is a function of salt concentration, and temperature. This scenario explained above is often not clearly delineated in scientific literature when compared to situations where the concentration of the dominant species within the solution is not uniform. Consider a case where salt is absent in the solution, but there are high concentrations of electroactive species present. In cases like this, $\gamma_i^c$ depends primarily on concentrations of these electroactive species rather than salt concentration. Because concentrations of electroactive species change considerably in the mass transfer domain, the activity term ($dln\gamma_i^c/dlnc_i$) in Eq. (9) cannot be ignored. Another example is when two solutions with different chemical compositions are separated by a permeable membrane, and diffusion occurs on both sides across the membrane. It's essential to emphasize that the scope of this review focuses on solutions with uniform compositions. With this context in mind, let's delve into the literature that covers the dependance of diffusivity ($D$) on temperature, pressure, and salt concentration.

### 4.1. Effect of pressure and temperature on diffusivity

The influence of pressure on species diffusion in a solution is typically minimal [122,126,169]. For species like $Na^+$ and $Cl^-$ ions in aqueous NaCl solutions, whose concentration remains unaffected by pressure due to the constant volume of aqueous solutions across various pressures, diffusivity remains steady regardless of pressure changes.[7] However, species like $CO_2$ and $H_2S$, whose concentrations are pressure-sensitive, experience higher diffusivity at elevated pressures, driven by increased concentrations in the solution [182]. On the other hand, as discussed earlier in this review, the dissolution of gases like $CO_2$ and $H_2S$ in water can elevate solution viscosity and this elevated viscosity, as will be shown shortly, hampers diffusivity. This sets up a

[5] In a broader perspective, the electrochemical potential ($Fz_i\Phi$), which results in the mass transfer by electromigration can be added to the definition of the chemical potential as follows: $\mu_i = \mu_i^0 + RTln(\gamma_i^c c_i) + Fz_i\Phi$; however, the electrochemical potential term gains significance in the context of dissolved ionic species and is usually neglected in aqueous chemistry calculations, particularly when no external electrical field is present.

[6] In the outlined derivation, two concentration units are employed: $c_i$ in molarity and $c_i^{'}$ in mol/cm$^3$, ensuring unit consistency across Eqs. 4, 5, and 7. Notably, the literature frequently overlooks this crucial unit consistency aspect.

[7] For pressures above the vapor saturation pressure of the solution.

delicate equilibrium between the enhancement of diffusivity due to higher concentration and the reduction of diffusivity due to increased viscosity. Consequently, the diffusivity of species like $CO_2$ and $H_2S$ remains relatively constant across different pressure conditions. This statement is supported by Fig. 4, which shows the diffusivities of dissolved $CO_2$ and $H_2S$ in water under varying pressure.

Temperature has a great influence on diffusivity. In search for an expression that describes the temperature effect, several models can be found in the literature [183–186]. The simplest of these models is given by the Stokes-Einstein equation [108,187,188], which relates species diffusivity to temperature and solution viscosity:

$$D^{o}_{T,i} = \frac{k_B T}{6\pi \mu_{T,w} R_i} \tag{11}$$

Here, $D^{o}_{T,i}$ is the diffusivity of species $i$ in $m^2/s$ at temperature $T$ in K and infinite dilution in water, $\mu_{T,w}$ is the viscosity of water in Pa.s, $k_B$ is the Boltzmann constant ($1.380649 \times 10^{-23}$ J/K), and $R_i$ is the radius of

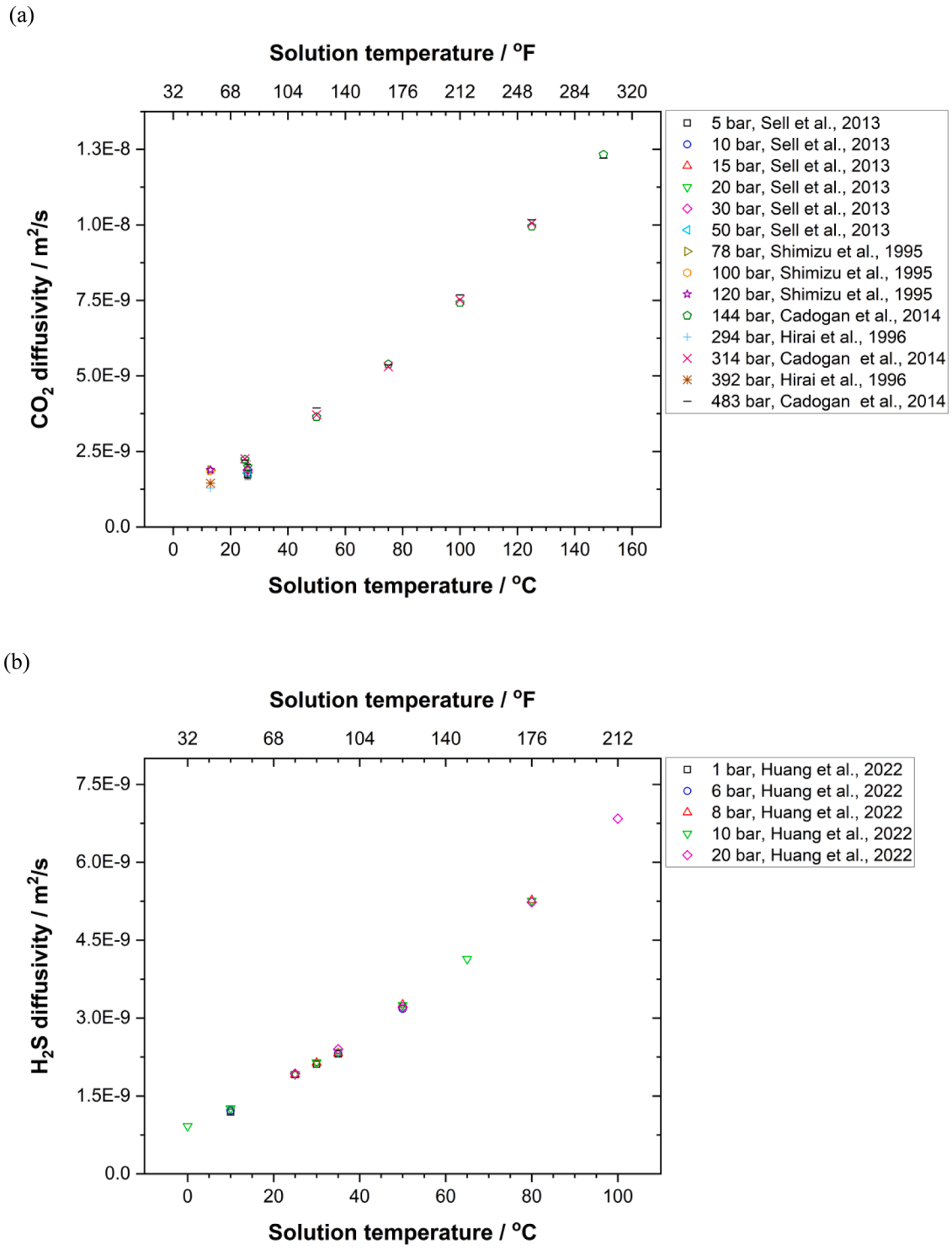


**Fig. 4.** Changes in diffusivities of (a) $CO_{2(aq)}$ and (b) $H_2S_{(aq)}$ in water at 25°C as a function of pressure. Experimental data points are borrowed from [122,126,158,169].

**Table 4**
Reference diffusivities at 25°C, 1 bar total pressure, and infinite dilution ($D^o_{298.15}$) of species commonly involved in aqueous weak acid corrosion of carbon steel.

| Species name | Species formula | $D^o_{298.15} \times 10^9$ ($m^2/s$) | Ref. |
|---|---|---|---|
| Hydrogen ion | $H^+$ | 9.312 | [108] |
| Sodium ion | $Na^+$ | 1.334 | [108] |
| Ferrous ion | $Fe^{2+}$ | 0.720 | [108] |
| Hydroxyl ion | $OH^-$ | 5.260 | [108] |
| Chloride ion | $Cl^-$ | 2.032 | [108] |
| Iodide ion | $I^-$ | 2.045 | [108,189] |
| Carbon dioxide | $CO_2$ | 1.953[a] | [116,129,132,133,138,139,141,142,146,148,190,191] |
| Carbonic acid | $H_2CO_3$ | 1.465[b] | This study |
| Bicarbonate ion | $HCO_3^-$ | 1.105 | [108] |
| Carbonate ion | $CO_3^{2-}$ | 0.804 | [115] |
| Hydrogen sulfide | $H_2S$ | 1.910[a] | [122,132,140] |
| Bisulfide ion | $HS^-$ | 1.731 | [192] |
| Sulfide ion | $S^{2-}$ | 0.842[c] | [193] |
| Acetic acid | $CH_3COOH$ | 1.201 | [124] |
| Acetate ion | $CH_3COO^-$ | 1.089 | [194] |
| Formic acid | HCOOH | 1.460 | [195] |
| Formate ion | $HCOO^-$ | 1.454 | [192] |
| Oxygen | $O_2$ | 2.120[a] | [146,141,116,196,151,144,168,197] |
| Hydrogen | $H_2$ | 4.220[a] | [116,144,154,196] |
| Nitrogen | $N_2$ | 1.960[a] | [144,160,198] |
| Methane | $CH_4$ | 1.850[a] | [154,199] |

[a] This is an average value calculated using data from the referenced literature selected for their reliable experimental methods and exhibiting little to no significant variation from one another.
[b] This value is calculated by using the modified Wilke and Change [183] equation proposed by Bidstrup and Geankoplis [200]. Carbonic acid is assumed to be a carboxylic acid with a Le Bas [201] molar volume of 49 $cm^3$/mol. The Le Bas molar volume for carbonic acid is obtained by adding 7.4 $cm^3$/mol which is the Le Bas molar volume of oxygen in the -OH structure to the Le Bas molar volume of formic acid, 41.6 $cm^3$/mol [200]. The calculated diffusivity for carbonic acid agrees well with the reported value by Krieg *et al.* [202]
[c] This is a calculated value from the measured diffusivity at 18°C, using the Stokes-Einstein Eq. (12).

hydrated species in m. Eq. (11) can be applied to correct the diffusivity at infinite dilution for the effect of temperature:

$$\frac{D^o_{T,i}}{D^o_{298.15,\ i}} = \frac{T}{298.15}\ \frac{\mu_{298.15,w}}{\mu_{T,w}} \tag{12}$$

$\mu_{298.15,w}$ is the viscosity of water at 298.15 K and $D^o_{298.15,\ i}$ is the diffusivity of species $i$ at 298.15 K and infinite dilution in water. It is noteworthy that the choice of units for diffusivity and viscosity in Eq. (12) is flexible. In studies of species diffusivity in aqueous solutions, it is a common practice to relate the diffusivity of species at different temperatures and concentrations to $D^o_{298.15}$. For practical illustration, a list of $D^o_{298.15}$ for species involved in aqueous weak acid corrosion of carbon steel is provided in Table 4.

In various instances within the open literature, Eq. (12) has been used to account for the effect of temperature on diffusivity of dissolved species [98,99,203,204]. However, Fig. 5 clearly shows that this equation fails to yield accurate results. Instead, an empirical equation proposed by Smolyakov, which relates the limiting conductance to temperature, is recommended in the present work [205]:

$$ln\left(\lambda^o_{T,i}\cdot\mu_{T,w}\right) = A + \frac{B}{T} \tag{13}$$

In Eq. (13), $T$ is the soluion temperature in K, $\lambda^0_{T,i}$ is the conductance of species $i$ at temperature $T$ and infinite dilution in water, $\mu_{T,w}$ is the dynamic viscosity of pure water at temperature $T$, and $A$ (dimensionless) and $B$ (in K) are adjustable constants which differ for each species. If Eq. (13) is combined with the Nernst-Einstein equation[8], and then the resulting equation is divided by itself at $T = 298.15$ K, the following equation is obtained that can be used to correct diffusivity for the effect of temperature:

$$\frac{D^o_{T,i}}{D^o_{298.15,\ i}} = \frac{T}{298.15}\ \frac{\mu_{298.15,w}}{\mu_{T,w}}\ \exp\left(\frac{B}{T} - \frac{B}{298.15}\right) \tag{14}$$

Eq. (14) has an extra exponential term compared to the Stokes-Einstein Eq. (12). The exponential term dampens (for positive $B$ constants) or amplifies (for negative $B$ constants) the temperature dependence of diffusivity. If $B$ is zero, Eq. (14) will be the same as Eq. (12). Both Eqs. (12) and (14) are originally derived for ionic species but have proven to be adaptable and effective for neutral species as well. Examples of successful application of Eq. (14) for neutral species $CO_{2(aq)}$, $H_2S_{(aq)}$, and $O_{2(aq)}$ can be seen in Fig. 5d, e, and f, respectively. It is worth noting that Eqs. (12) and (14) can also be applied to correct diffusivity of salt solutions for temperature effect, by substituting the viscosity of solution ($\mu_{sol}$) in place of that for water ($\mu_w$). Table 5 provides $B$ values for various species, and for additional species, readers can refer to the literature [205,206]. No data could be found for weak acids except for acetic acid, where a linear relationship between diffusivity and temperature was reported [200], suggesting that $B$ should be equal to zero. The same was reported for carboxylic acids [183,184,200]. By analogy, it can be assumed that weak carbonic acid and its dissociated ions also exhibit a linear temperature dependence, as indicated in Table 5.

Fig. 5 visually demonstrates a strong agreement between the diffusivities obtained with the Smolyakov equation Eq. (14) and the experimental data sourced from the literature. The diffusivity of species such as $H^+$ ion and $H_2S_{(aq)}$ exhibited a strong match with the experimental data when characterized by a positive $B$ value, while for species like $O_{2(aq)}$ and $CO_{2(aq)}$ the match could be obtained with a negative $B$ value.

### 4.2. Effect of salt concentration on diffusivity

The concentration dependency of diffusivity in electrolyte solutions has been extensively investigated. In dilute electrolyte solutions, the change in diffusivity of electroactive species with salt concentration is

[8] The Nernst-Einstein equation for ionic species [108]: $D_i = \frac{RT\lambda_i}{|z_i|F^2}$ where, $D_i$ is the diffusivity of dissolved species $i$ in the solution in $m^2/s$, $R$ is the gas constant in J/mol/K, $T$ is temperature in K, $\lambda_i$ is the conductance of species $i$ in $S.m^2/mol$ at temperature $T$, $z_i$ is the charge number of species $i$, and $F$ is the Faraday constant in C/mol.

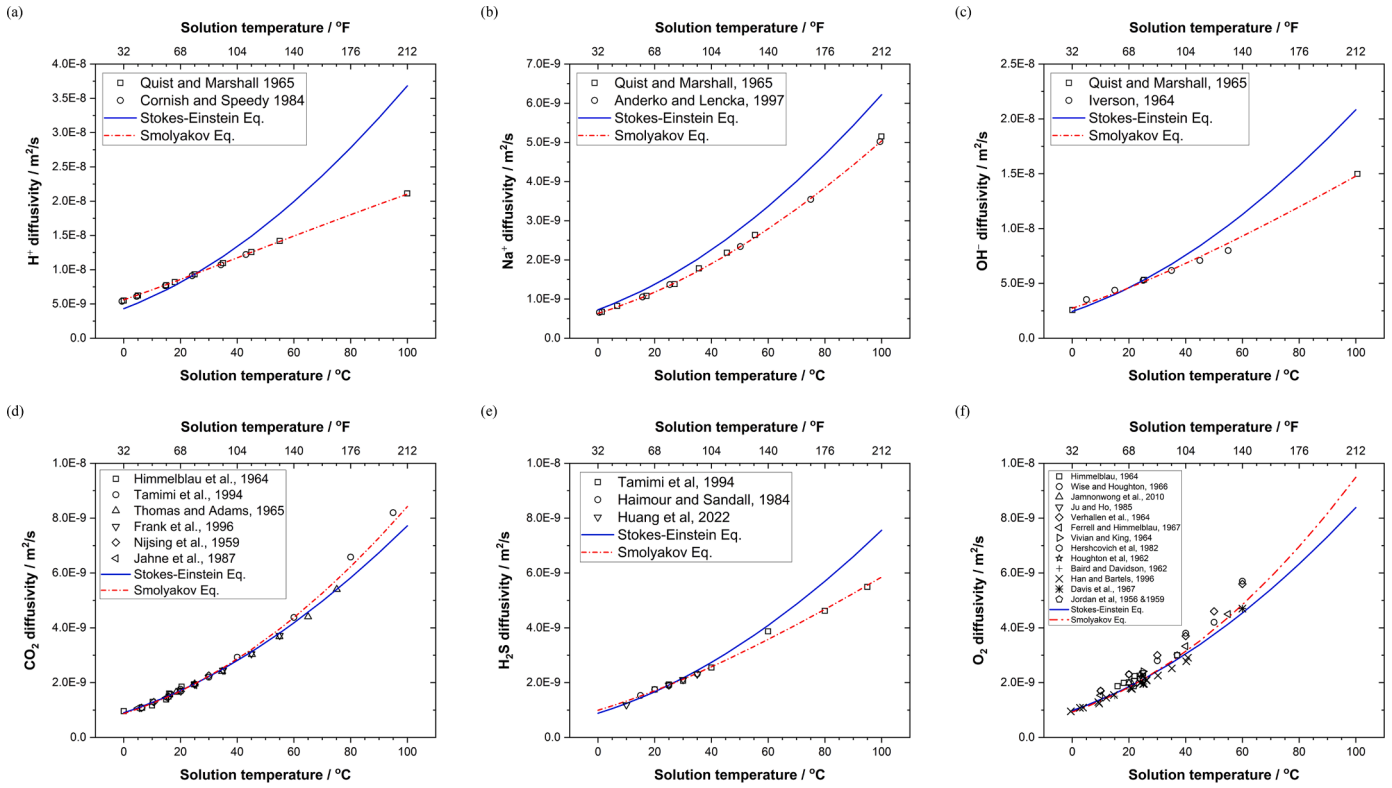


**Fig. 5.** Performance evaluation of the Stokes-Einstein Eq. (12) and the Smolyakov Eq. (14) for correcting diffusivity at infinite dilution in water for the effect of temperature by comparing the calculated diffusivities (lines) with experimental data (points) from the literature [148,138,132,139,140,205,165,170,166,207,119]: (a) $H^+$ ion, (b) $Na^+$ ion (c) $OH^-$ ion, (d) $CO_{2(aq)}$, (e) $H_2S_{(aq)}$, and (f) $O_{2(aq)}$.

**Table 5**
Values of *B* used in Eq. (14) for calculating the temperature dependence of diffusivity for selected key species in aqueous corrosion and electrochemical studies.

| Species name | Species formula | $B^a$ | Ref. | Experimental data source |
|---|---|---|---|---|
| Hydrogen ion | $H^+$ | 837.790 | [205] | [166,207] |
| Sodium ion | $Na^+$ | 75.492 | [205] | [205,207] |
| Hydroxide ion | $OH^-$ | 468.130 | [205] | [165,207] |
| Chloride ion | $Cl^-$ | 216.030 | [205] | N/A |
| Carbon dioxide | $CO_2$ | -129.120 | This study | [132,138,148,170] |
| Carbonic acid | $H_2CO_3$ | 0 | This study | N/A |
| Bicarbonate ion | $HCO_3^-$ | 0 | This study | N/A |
| Carbonate ion | $CO_3^{2-}$ | 0 | This study | [115,193] |
| Hydrogen sulfide | $H_2S$ | 379.400 | This study | [122,132,140] |
| Bisulfide ion | $HS^-$ | 0 | This study | [193] |
| Sulfide ion | $S^{2-}$ | 0 | This study | [193] |
| Acetic acid | CHCOOH | 0 | This study | [200] |
| Acetate ion | $CHCOO^-$ | 0 | This study | N/A |
| Formic acid | HCOOH | 0 | This study | N/A |
| Formate ion | $HCOO^-$ | 0 | This study | N/A |
| Oxygen | $O_2$ | -185.480 | This study | [146,141,196,151,144,197] |
| Methane | $CH_4$ | 387.620 | This study | [154,186,199] |

[a] It has the unit of temperature, Kelvin.

associated with two long-range (coulombic) ionic interactions known as *relaxation* and *electrophoretic* effects [208]. Debye and Huckel were the first to identify these two effects [209,210]. The relaxation effect represents the return to equilibrium (local electroneutrality) after a distortion in the ionic atmosphere (fixed background of solution) due to the movement of diffusing ion [40,206,208,210,211]. The electrophoretic effect is related to the decrease in the motion of the diffusing species because of the countermotion of solvent in the ionic atmosphere [40,208,210–212]. In the case of self-diffusion of electroactive species in the presence of a supporting electrolyte, which is the focus of this review, there is no significant countermotion of the solvent and the electrophoretic effect can be considered to be negligible [211].

In concentrated electrolyte solutions the role of interparticle short-range interactions, such as those between ion-ion, ion-dipole, ion-induced dipole, induced-dipole-induced dipole, becomes increasingly significant in the estimation of diffusivity. These short-range interactions depend on the crystallographic diameter of diffusing species as well as its solvation structure. Wang and Anderko [213] modeled the contribution of short-range interactions on diffusivity by using the hard-sphere theory. In electrolyte solutions, diffusivity is predominantly influenced by long-range electrostatic Coulombic interactions, a phenomenon observed up to concentrations of around 1 M [206,214].

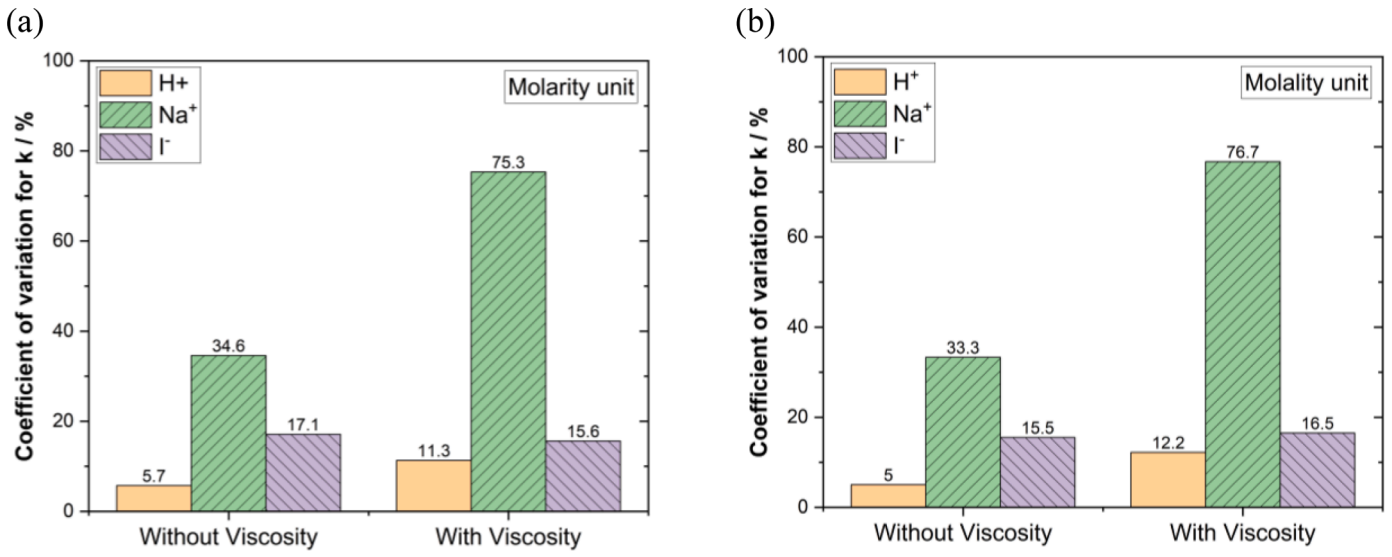


**Fig. 6.** Comparison of coefficient of variation for $k$ in assessing the accuracy of the square root Eq. (16) (without viscosity) and the modified square root Eq. (17) (with the viscosity term) for the concentration dependency of diffusivity: (a) with molarity unit (M), (b) with molality unit (m). Experimental diffusivity data for $H^+$ ion (19 measurements), $Na^+$ ion (5 measurements), and $I^-$ ion (12 measurements) at 25°C, atmospheric pressure, and various concentrations are taken from [110, 114,211,221].

**Table 6**
The $k$ value used in the square root Eq. (16) for correcting the diffusivity of aqueous species for the effect of NaCl concentration.

| Species name | Species formula | $k$ $(mol/lit)^{-0.5}$ | $k$ $(mol/kgH_2O)^{-0.5}$ | Ref. | Experimental data source |
|---|---|---|---|---|---|
| Hydrogen ion | $H^+$ | 0.277 | 0.273 | This study | [110,114,211] |
| Hydrogen ion | $H^+$ | 0.21 | N/A | [219] | N/A |
| Hydrogen ion | $H^+$ | 0.256 | N/A | [222] | N/A |
| Sodium ion | $Na^+$ | 0.133 | 0.129 | This study | [110,124,211] |
| Chloride ion | $Cl^-$ | 0.172 | 0.166 | This study | [110,211,226] |
| Iodide ion | $I^-$ | 0.179 | 0.173 | This study | [110,211,221] |
| Carbon dioxide | $CO_2$ | 0.147 | 0.142 | This study | [190] |
| Carbonic acid[a] | $H_2CO_3$ | 0.147 | 0.142 | This study | N/A |
| Hydrogen sulfide | $H_2S$[b] | 0.118 | 0.116 | This study | [122,143] |
| Oxygen | $O_2$ | 0.161 | 0.156 | This study | [121,156,157] |

[a] Assume to be the same as $CO_2$.
[b] The Stokes-Einstein Eq. (15) provides more accurate diffusivity predictions for $H_2S$.

Therefore, as an initial approximation, it is common practice to disregard the effects of short-range interactions in such scenarios. However, it is important to note that at concentrations exceeding approximately 1 M, the contribution of the short-range interactions becomes notably significant [206].

Experimental observations consistently indicate that, as a general trend, diffusivity tends to decrease as salt concentration increases [110, 215]. However, the extent of this decrease depends on the nature of the salt and the diffusing species. For example, when examining the decrease in diffusivity of $Cl^-$ ion in various salt solutions, it follows this order in terms of magnitude: KCl < NaCl < LiCl [215]. There are some exceptions, for instance, diffusivity of $Cl^-$ ion in aqueous CsCl solutions first decreases and then increases with increasing CsCl concentration [215]. The analysis of this complex behavior is beyond the scope of the current paper. Instead, the focus will be directed towards the common decreasing trend observed in diffusivities.

Several equations and models have been proposed to correct diffusivity with respect to salt concentration in aqueous salt solutions. The simplest method, similar to how temperature effect is handled, involves using the Stokes-Einstein Eq. (12), in which the variation of diffusivity is tied to that of viscosity [108]:

$$\frac{D_{T,i}}{D^o_{T,i}} = \frac{\mu_{T,w}}{\mu_{T,sol}} \tag{15}$$

Here, $D_{T,i}$ and $\mu_{T,sol}$ are the diffusivity of species $i$ and the dynamic viscosity of the aqueous solution at a given salt concentration and temperature $T$, respectively, $D^o_{T,i}$ is the diffusivity of species $i$ at temperature $T$ and infinite dilution in water (calculated from Eq. (14)), and $\mu_{T,w}$ is the dynamic viscosity of water at temperature $T$. Due to its simplicity, Eq. (15) has found frequent use in the literature [216–218]. However, as will be shown later, Eq. (15) has the correct trend but is rather inaccurate in capturing the variation in the diffusivity of species with salt concentration.

Another approach frequently used in the literature [114,156, 219–222] is an empirical correlation with a square root dependency of the diffusivity on salt concentration, The simplest form of this correlation for a univalent salt solution (*e.g.*, NaCl, Kl, *etc.*) is:

$$\frac{D_{T,i}}{D^o_{T,i}} = 1 - k\sqrt{c} \tag{16}$$

where, $D_{T,i}$ and $D^o_{T,i}$ have been previously defined, $c$ is the concentration of salt in the solution, usually expressed as molarity (M), and $k$ is a constant that depends on the nature of the dissolved salt and the diffusing species. Eq. (16) is known as the *square root* equation. The unit for $k$ is the reciprocal of the square root of the concentration unit. In some cases, especially when dealing with polyvalent salts or multiple salts dissolved in the solution, concentration ($c$) is replaced with ionic

strength ($I$) [109,156].

Eq. (16) is reported to be valid for very dilute solutions, up to ~0.03 M [223]. Several modifications have been proposed for Eq. (16) to extend its validity range to higher concentrations or enhance its accuracy [220,221,223–225]. For instance, Stastny and Strafelda [220] used the cube root of salt concentration for aqueous KCl solutions, $D^o_{T,i}(1 - k(c_{KCl}/c_{H^+})^{1/3})$. Alternatively, Stokes *et al.* [221] suggested using $1/(1+\kappa a)$ or $1/\left[(1+\kappa a)\left(1+\frac{\kappa a}{\sqrt{2}}\right)\right]$ instead of the constant $k$ to enhance the accuracy of Eq. (16). Here, $\kappa$ represents the reciprocal Debye length in 1/m and $a$ is the Debye-Huckel ion-size parameter in m. However, Stokes *et al.* [221] did not show the results of the implementation of this equation in their publication. Nevertheless, it has been shown in the present article that Eq. (16), without any modifications, can be used rather successfully to predict diffusivity even in significantly concentrated brine solutions.

Given that diffusive transport of mass and viscous transport of momentum are analogous, both depending on molecular properties of the solution [114,181,211], there have been suggestions that combining Eqs. (15) and (16) by multiplying the right-hand side of Eq. (16) by a viscosity term of $\mu_{T,w}/\mu_{T,sol}$, could improve the prediction accuracy [111, 114,221,222]. Nonetheless, it becomes evident that utilizing this method leads to double-counting of the effect of concentration, first directly through Eq. (16), and then indirectly through viscosity, which itself is concentration-dependent, as shown by Eq. (1). This has been previously reported, where the addition of the viscosity term to Eq. (16) overcorrected the effect of concentration on diffusivity [211,221]. To address this issue, Pinto and Graham [211] argued that the viscosity term should be introduced into Eq. (16) with an exponent of 0.7 instead of 1, resulting in a modified Eq. (16) in the following form:

$$\frac{D_{T,i}}{D^o_{T,i}} = (1 - k\sqrt{c})\left(\frac{\mu_{T,w}}{\mu_{T,sol}}\right)^{0.7} \tag{17}$$

It is worthwhile to assess whether addition of the viscosity term truly improves the diffusivity estimation or if Eq. (16) performs adequately on its own. To investigate this, the following approach was employed: for a given species ($H^+$, $Na^+$, and $I^-$ in this study), $k$ is back-calculated using Eq. (16) and Eq. (17) based on experimental data. The equation that results in $k$ values with least deviation can be considered the most appropriate for accurately correcting the diffusivity. The *coefficient of variation*[9] is used as an indication of the degree of scatter in $k$. Fig. 6a and b provide a comparison between the two equations, using molarity and molality concentration units, respectively. The deviation of $k$ for Eq. (16) is generally smaller than that for Eq. (17), implying that introducing the viscosity term is unnecessary and Eq. (16) is sufficient for describing the concentration dependency of diffusivity.

The choice between molality and molarity in Eq. (16) has only a marginal impact on the resulting diffusivity value. In some cases, the use of molality units may yield slightly more accurate results, while in other instances, molarity units may be equally effective, as indicated in Fig. 6 and Table 6. Regardless, the difference in accuracy when using these two concentration units is minimal. As a result, either molarity or molality can be employed in Eq. (16) to correct diffusivity for the effect of salt concentration. In general, molality is preferred over molarity for two key reasons. First, calculation of molality does not rely on solution density, simplifying practical applications. Secondly, molality stands as the predominant concentration unit in aqueous solution chemistry models found in the literature, ensuring consistency and compatibility with previous research.

Table 6 shows the calculated $k$ values for various species, derived by fitting the square root Eq. (16) to experimental data gathered from the literature. Among the species listed in Table 6, only the $k$ value for $H^+$ ion was found in the open literature, allowing for a direct comparison [219,222]. This comparison resulted in a favorable match, thus affirming the credibility and reliability of the methodology employed in this study. In Stackelberg and Pilgram's [219] work a $k$ value of 0.21 was reported for $H^+$ ion diffusivity in KCl aqueous solutions, while Ciskowska *et al.* [222] used a $k$ value of 0.256 for the diffusivity of $H^+$ ions in $LiClO_4$ salt solutions.

Another model that addresses the concentration dependency of diffusivity was proposed by Appelo [227] and has been integrated into a software package called PHREEQC. This model seems to be based on the Stokes *et al.*'s [221] correction, as mentioned earlier, and it extends a simpler model previously presented by Snyder *et al.* [228]. Much like Eq. (16), the concentration dependency term in Appelo [227] model has the square root of ionic strength (or concentration for 1:1 salts); however, it is placed inside an exponential function to dampen the changes in diffusivity with varying salt concentration. The main equation in the Appelo [227] model that contains the concentration dependency is shown below:

$$D_{T,i} = D^o_{T,i}\exp\left(\frac{-a_{1i}A|z_i|\sqrt{I_s}}{1+\kappa a}\right) \tag{18}$$

Here, $D_{T,i}$ and $D^o_{T,i}$ have been previously defined, $I_s$ is the ionic strength of solution, $A$ is the Debye-Huckel parameter in $(kg/mol)^{0.5}$, $\kappa$ is the Debye-Huckel reciprocal length in 1/m, $a$ is the ion-size parameter for species $i$ in m, $z_i$ is the charge number of species $i$, and $a_{1i}$ is an empirical coefficient for species $i$.

There are several concerns regarding the implementation of the Appelo [227] model.[10] Firstly, there is inconsistency in the unit of ionic strength (molality *vs.* molarity) used in the Appelo's [227] publication, which can complicate model's replication. Secondly, the range of validity of the Appelo model with respect to salt concentration is not clearly specified; however, from the graphs in the publication, [227] it appears to be limited to 2 molal, which is relatively narrow. Additionally, the number of species covered by the Appelo model is limited, which makes the model less practical for different applications. Lastly, the Appelo model [227] does not work for neutral species, such as undissociated $H_2CO_3$, $H_2S$, and carboxylic acids. Nevertheless, the Appelo model [227] is reproduced in this study and compared with other models for its accuracy, as shown in Fig. 7.[11]

A more complex model for the estimation of diffusivity in concentrated solutions was proposed by Pinto and Graham [111,211]. The final equation in this model that relates the diffusion coefficient to concentration of dissolved ionic species takes the following form [111,211]:

$$D_{T,i} = \frac{1}{\frac{x_0}{a_{i0}} + \sum_{\substack{j=1 \\ j\neq i}}^{n} \frac{x_j}{a_{ij}}} \tag{19}$$

where, $D_{T,i}$ is already defined, $a_{i0}$ is the ion-solvent interaction coefficient, $a_{ij}$ is the Stefan-Maxwell phenomenological coefficient, $x_0$ is the mole fraction of water (solvent), $x_j$ is the mole fraction of ionic species $j$, and $n$ is the number of ionic species in the solution. The ion-solvent interaction coefficient is given by:

[9] The coefficient of variation (CV) is defined as the ratio of the standard deviation to the mean. It is often expressed as a percentage.

[10] The units for the Debye-Huckel reciprocal length ($\kappa$), ion-size parameter ($a$), and the Debye-Huckel parameter ($A$) are reported incorrectly in the publication. The correct equation for A is as follows: $A = 3A_\phi/\ln(10)$ in $(kg/mol)^{0.5}$, where $A_\phi$ is the Debye-Huckel parameter for osmotic coefficient (0.391 at 1 bar and 25°C) [229,230]. Furthermore, the equation stated as (28) in the Appelo [227] publication is incorrect. The correct equation can be found in ref. [231] and in the PHREEQC software database.

[11] In this study, molarity (m) is considered for replicating the Appelo [227] model.

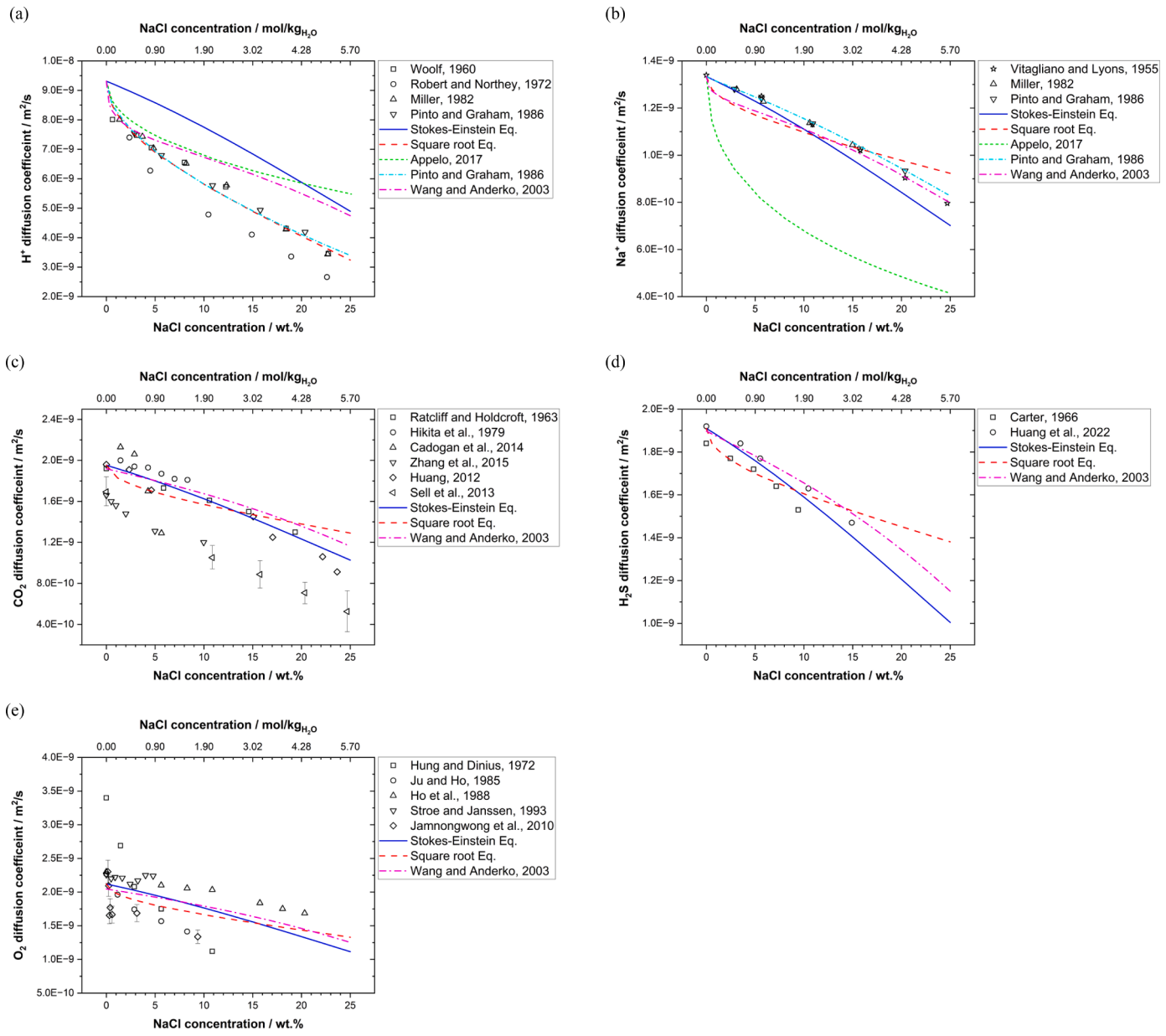


**Fig. 7.** Performance assessment of models for the concentration dependency of diffusivity in aqueous NaCl solutions at 25°C and atmospheric pressure by comparing the calculated diffusivities (lines) with experimental data (points) from the literature: (a) $H^+$ ion, (b) $Na^+$ ion, (c) $CO_{2(aq)}$, (d) $H_2S_{(aq)}$, and (e) $O_{2(aq)}$. The "Stokes-Einstein Eq." and the "Square root Eq." represent Eqs. (15) and (16), respectively. Experimental data are taken from [211,110,169,126,122,190,114,226,143,156,121,157,155,232,118,117,167,123].

$$a_{i0} = D^o_{T,i}\, x_0 \left(\frac{\mu_{T,w}}{\mu_{T,sol}}\right)^{0.7} \tag{20}$$

The Stefan-Maxwell coefficients for ionic species interactions are given by:

$$a_{ij} = -\frac{2D^o_{T,i}\, D^o_{T,j}}{D^o_{T,i}\,|z_i| + D^o_{T,j}\,|z_j|}\left[\frac{A\sqrt{x_I}}{1+\sqrt{x_I}}\right]\left(\frac{\mu_{T,w}}{\mu_{T,sol}}\right)^{0.7} \tag{21}$$

when ions $i$ and $j$ have the same type of charge (both positive or both negative), or by:

$$a_{ij} = +\frac{D^o_{T,i}\, D^o_{T,j}}{D^o_{T,i}\,\nu_i + D^o_{T,j}\,\nu_j}\left[\frac{A\sqrt{x_I}}{1+\sqrt{x_I}}\right]\left(\frac{\mu_{T,w}}{\mu_{T,sol}}\right)^{0.7} \tag{22}$$

when ions $i$ and $j$ are of opposite charge. Here, $\mu^o_{T,i}$ and $\mu_{T,i}$ have been introduced earlier, $A$ is called the ternary constant indicating the distance of minimum approach between ion pairs, $z$ is the charge number of ionic species, $\nu$ is the stoichiometric number of ionic species in the form of an undissociated salt, $x_I$ is the total mole fraction of all species present in the solution (equal to $1 - x_0$).

The Pinto and Graham [211] model uses an analogy between the Stefan-Maxwell flux equation and the Fick's law of diffusion, and therefore connects the diffusivity to the Stefan-Maxwell phenomenological coefficients. The model only considers the relaxation effect and assumes that electrophoretic effect is negligible, which is an acceptable assumption for self-diffusion scenarios, as explained earlier. Additionally, Pinto and Graham [211] assumed that the distance of minimum approach between pairs of ions, involving one specific ion combined with other ions, is constant, which is only valid if the size of dissolved ionic species do not differ considerably. Another assumption in the original Pinto and Graham model is that all ions are considered to be

completely non-hydrated. Later, they included the hydration number in the diffusivity calculations [111], significantly increasing its complexity. However, the equations and parameters required to reproduce the updated model are not clearly described in their latest publication [111]. Thus, reproducing the updated Pinto and Graham model [111] becomes a challenging endeavor.

Similar to the limitations discussed in the Appelo model [227], the Pinto and Graham model [111,211], also faces constrains. It is not applicable to neutral species, restricting its utility in certain scenarios. Additionally, the phenomenological coefficients are provided only for four species ($H^+$, $Na^+$, $Cl^-$, $I^-$), limiting a broader applicability of the model. Therefore, only the original Pinto and Graham [211] model is reproduced in this study and compared with other models, as presented in Fig. 7.

The most elaborate model available in the literature for accounting for the effect of salt concentration on diffusivity is proposed by Wang and Anderko [213]. They included the effects of both long-range electrostatic forces (relaxation effect) and short-range forces (due to interparticle interactions) in their model. They claimed that without considering the short-range interactions, the model for univalent ions is only valid up to ~1 M of salt concentration, while with the short-range interactions included in the model the validity range expands to ~ 30 m [206]. Another apparent advantage of the Wang and Anderko [213] model claimed by the authors, is that it covers the effect of salt concentration on diffusivities of both ionic and neutral species [213]. This model is therefore much more complicated than the other models discussed above. More importantly, not all the equations and parameters required to replicate the model are provided in their publications [206, 213]. Therefore, the Wang and Anderko [213]. model is impossible to reproduce. For comparing the accuracy of the Wang and Anderko model [213] with abovementioned models, the diffusivity was obtained by running the commercial software package, OLI Studio in which the Wang and Anderko [213]. model is implemented. Now that five established models for calculating diffusivity as a function of salt concentration have been discussed, let's proceed to compare their performance for five different species as shown in Fig. 7. The Appelo [227] model and the original Pinto and Graham [211] model do not account for neutral species, so no line exists for these models for neutral species in Fig. 7.

Fig. 7a shows the comparison between the models for $H^+$ ion diffusivity in aqueous NaCl solutions. Of the four sets of experimental data found in the literature and used for comparison, the one reported by Roberts and Northey [155] is considered as outliers, and thereby, is not used to judge the accuracy of the models. Of the five models compared in Fig. 7a, the Stokes-Einstein Eq. has the least accuracy when calculating $H^+$ ion diffusivity. The accuracy for the Appelo [227] and the Wang and Anderko [213] models is similar, agreeing with the experimental data at low NaCl concentrations (up to about 3 wt.%), with significant deviations at moderate and high NaCl concentrations. On the other hand, the square root Eq. and the Pinto and Graham [211] models show nearly identical accuracy with a very strong agreement with the experimental data.

For the diffusivity of $Na^+$ ion shown in Fig. 7b, the Appelo [227] model predictions exhibit substantial deviations. The Stokes-Einstein Eq. slightly exaggerates the influence of salt concentration on $Na^+$ ion diffusivity and this exaggeration becomes more pronounced as NaCl concentration rises. The square root Eq. slightly underpredicts $Na^+$ ion diffusivity for NaCl concentrations below 15 wt.% and overpredicts for higher NaCl concentrations. The Wang and Anderko [213] model behaves similarly to the square root Eq. for NaCl concertation below 15 wt. %, but aligns well with the data for concentrations beyond this range. Finally, the Pinto and Graham [211] model shows almost prefect predictions for $Na^+$ ion diffusivity across the entire range of NaCl concentrations.

When it comes to the diffusivity of aqueous $CO_2$, a neutral species, the comparison is shown in Fig. 7c. The experimental data can be divided into two distinct sets, four datasets (Ratcliff and Holdcroft [190], Hikita *et al.* [118], Cadogan *et al.* [169], and Huang *et al.* [122]) consistently report higher values compared to the other two datasets (Zhang *et al.* [123] and Sell *et al.* [126]). All three models agree with the first group of experimental data. For the lack of a better criterion, this broad alignment between the four experimental datasets and the three independent models is used to eliminate the other experimental data from the analysis. Across a broad range of salt concentrations, the three models for $CO_2$ diffusivity performed equally well, with the Stokes-Einstein Eq. demonstrating a slightly superior fit to the experimental data, particularly in the high concentration range.

The change in diffusivity of aqueous $H_2S$, also a neutral species, with salt concentration is shown in Fig. 7d. The two available experimental datasets are in reasonable agreement with each other, and the three models show equally good alignment with the experimental results. Similar to $CO_2$, the Stokes-Einstein Eq. appears to provide more accurate predictions, especially in the high salt concentration range.

Finally, for diffusivity of aqueous oxygen, the experimental data found in the literature exhibit a considerable degree of scatter. Even in pure water the values differ considerably between different studies. One dataset stands out as clear outlier (Hung and Dinius [117]) and consequently will not be used for comparisons with the models. The remaining data still significantly differ from each other, even when considering studies conducted by the same research group but separated by a few years (Ju and Ho [156] and Ho *et al.* [157]). The predictions made by the three models pass in between the scattered experimental datasets with a consistent trend and similar levels of accuracy.

In summary, the Pinto and Graham [211] model demonstrates the best performance in predicting the diffusivity of the ionic species $H^+$ and $Na^+$ ions; however, its biggest drawback is that it does not work for neutral (uncharged) species. For the neutral species the argument can be made that the Stokes-Einstein Eq. (15) performs the best, yet its prediction of diffusivity of ionic species is inferior compared to certain other models. Taking into account the simplicity of the square root Eq. (16) and its applicability to both ionic and neutral species, coupled with its relatively good accuracy across the tested scenarios, it is the model recommended in this study for correcting the diffusivity of dissolved species for the effect of salt concentration.

Having discussed the impact of salt concentration on three key solution properties—density, viscosity, and diffusivity—and identified the most effective models for each, it is time to put these models into practical use. An excellent example to test these models is by predicting the electrochemical limiting current density which is a measurable parameter that relies on all three properties: the density and viscosity of the solution, as well as the diffusivity of electroactive species. In the upcoming sections, the experimental methodology employed to measure the limiting current density for $H^+$ reduction reaction will be explored. The $H^+$ ion limiting current density holds immense importance across various fields, including electrolysis and hydrogen production, fuel cell technology, electroplating processes, battery research, water purification methods, and corrosion studies. Subsequently, a comparison between the experimental values and calculated values, utilizing a comprehensive model that accounts for the influence of salt concentration on all three properties, will be conducted. This approach allows for the assessment of the model's performance in a real-world scenario.

## 5. Experimental methods

Strong acid solutions, saturated with an inert gas, can be considered as one of the simplest types of aqueous solutions used for $H^+$ ion limiting current density measurements, because the main electrochemical reaction in these solutions, across a broad potential range, is the $H^+$ ion reduction reaction. On the other hand, in weak acid solutions, which may contain substances like $H_2CO_{3(aq)}$ $H_2S_{(aq)}$ or carboxylic acids, interfering homogenous chemical reactions can alter the magnitude of the $H^+$ ion limiting current density by the buffering effect [233]. As a result, weak acid solutions are not suitable for the specific objective of

investigating the effect of salt concentration on density, viscosity, and diffusivity.

Two sets of experiments were carried out at 10°C and 20°C and different NaCl concentrations in $N_2$-saturated aqueous NaCl solutions. Precise temperature control, with an accuracy of within 0.5°C, was achieved by employing a combination of a cooling apparatus and a hot plate. In addition to the standard room temperature of 20°C, a lower solution temperature of 10°C was selected for the experiments. This choice was made because, at lower temperatures, the rate of charge transfer reactions at the metal surface is significantly slower than the rate of diffusive mass transfer of electroactive species to the electrode surface. This disparity in reaction rates makes it simpler to distinguish between the charge transfer and limiting current density regions in cathodic potentiodynamic sweeps, consequently enhancing the accuracy of extracting the limiting current density from the sweeps.

A conventional three-electrode setup was used for performing the limiting current density measurements. In separate experiments, two types of working electrodes were used: rotating disk electrode (RDE) and rotating cylinder electrode (RCE) for accurate control of mass transfer rates in laminar and turbulent flow regimes, respectively. The RDE was rotated at 2000 rpm in a laminar flow regime. The RCE rotation speed was 1000 rpm in a turbulent flow regime. A saturated Ag/AgCl electrode was used as a reference electrode and the counter electrode was a platinized titanium mesh with dimensions 20 × 30 $mm^2$. The working electrode was made out of API 5L X65 mild steel, a commonly used steel grade in the oil and gas industry for pipeline manufacturing. The microstructure of the X65 mild steel was a uniform, fine structure of pearlite in a ferrite matrix. The chemical composition and microstructure of X65 steel are given elsewhere [109]. The RDE diameter was 5.0 ± 0.1 mm, with an area of 0.196 $cm^2$. The RCE dimensions were 11.9 ± 0.1 mm OD and 14.0 ± 0.1 mm length, which gave an exposed surface area of 5.4 $cm^2$. The working electrodes were sequentially wet polished with 240-, 400- and 600-grit abrasive papers followed by ultrasonically degreasing with isopropanol for 3 min and dried in cool $N_2$ gas prior to immersion in the test solution.

Experiments were done at five NaCl concentration of 0.1, 1, 3, 10, and 20 wt.% using each electrode type. Each experiment was repeated at least two times to ensure the reliability of results. For each experiment, NaCl was dissolved in deionized water (18 MΩ.cm) in a 2-liter glass cell. The solution was then sparged with $N_2$ gas for at least 2 h, while being stirred. When a stable pH was achieved ($\Delta pH < 0.01$), 0.1 M HCl stock solution was added gradually to the main solution to adjust pH at 3.0. After that the freshly polished specimen was inserted into the solution and its open circuit potential (OCP) was monitored until a stable value ($\Delta E_{OCP} <$ 2 mV/min) was achieved. Then, electrochemical impedance spectroscopy (EIS) was carried out in a frequency range of 10,000 Hz to 0.1 Hz at OCP with a 10 mV AC peak to peak amplitude and a sampling rate of 8 points/dec to determine the solution resistance (iR drop). Finally, a cathodic potentiodynamic (PD) polarization sweep was performed starting from the OCP toward more negative potentials up to -1.00 V vs OCP, using a scan rate of 0.5 mV/s. The measured values were corrected for the solution resistance. A Gamry Reference 600 potentiostat was used for all the electrochemical measurements. A more detailed description of the experimental procedure with pictures of the experimental equipment, setup, electrodes, *etc.* is given by Madani Sani [109].

## 6. Comparison of the experimental and calculated limiting current densities

Fig. 8 shows the comparison between the experimental limiting current density (dots) and the calculated limiting current density (solid black line), at different NaCl concentrations for each electrode type. The limiting current densities for RDE and RCE electrodes were calculated by using the Levich [106,234,235] and Eisenberg [236,237] equations, respectively.

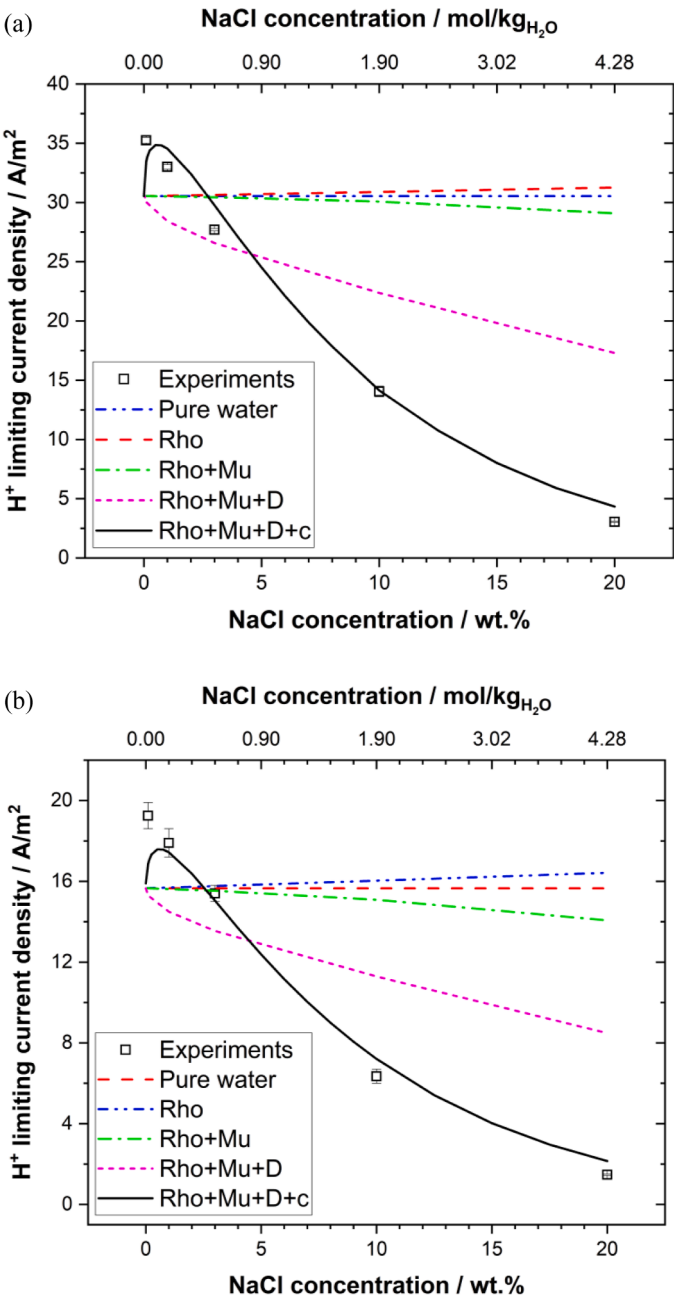


**Fig. 8.** The comparison between the experimental (dots) and calculated (lines) $H^+$ limiting current density ($i_{Lim}$) values for (a) RDE electrode setup at 10°C, 1 bar $N_2$ gas, pH 3, and 2000 rpm and (b) RCE electrode setup at 20°C, 1 bar $N_2$ gas, pH 3, 1000 rpm. The "Pure water" shows $i_{Lim}$ for pure water conditions. The "Rho", "Rho+Mu", "Rho+Mu+D", "Rho+Mu+D+c" lines are calculated $i_{Lim}$ when the effect of NaCl concentration is applied cumulatively to solution density (Rho), solution viscosity (Mu), $H^+$ diffusivity (D), and $H^+$ ion concentration (c).

$$i_{Lim,\ RDE} = 200.635nF(rpm)^{0.5}\rho^{0.167}\mu^{-0.167}D^{0.667}c_b \quad (23)$$

$$i_{Lim,RCE} = 10.034nFd^{0.4}(rpm)^{0.7}\rho^{0.344}\mu^{-0.344}D^{0.644}c_b \quad (24)$$

where, $i_{Lim}$ is the limiting current density in A/$m^2$, $n$ is charge number of reacting ion, $F$ is the Faraday constant (96485.33 C/mol), $rpm$ is the rotational speed of the electrode in revolutions per min, $d$ is the diameter of electrode in m, $\rho$ is the solution density in kg/$m^3$, $\mu$ is the solution viscosity in kg/m/s, $D$ is the diffusivity of reacting ion in $m^2$/s and $c_b$ is

the bulk concentration of reacting ion in M. The reacting ion in these experiments is $H^+$ ion.

The NaCl solution density ($\rho$) was calculated with the Novotny and Sohnel [45,46] model:

$$\rho = \rho_w + 44.85c_s - 0.09634c_s t + 0.0006136c_s t^2 - 2.712c_s^{1.5} + 0.01009c_s^{1.5} t \quad (25)$$

$$\rho_w = 999.65 + 0.20438t - 0.06174t^{1.5} \quad (26)$$

where, $\rho_w$ is the density of water in kg/m$^3$, $t$ is the solution temperature in °C, and $c_s$ is the NaCl concentration in molarity. The conversion from various concentration units to molarity is given in Appendix A of Madani Sani [109].

The NaCl solution viscosity ($\mu$) was computed with the Mao and Duan [65] model:

$$\mu = \mu_w \exp\left(Am_s + Bm_s^2 + Cm_s^3\right) \quad (27)$$

where, $\mu_w$ is the viscosity of water in kg/m/s, and $A$, $B$, and $C$ are empirical polynomial functions of temperature. The equations for $\mu_w$, $A$, $B$, and $C$ are given in Mao and Duan [65].

The diffusivity of $H^+$ ion was calculated using the square root Eq. (16):

$$D_{H^+} = D^o_{H^+}(1 - 0.273\sqrt{c_s}) \approx D^o_{H^+}(1 - 0.273\sqrt{m_s}) \quad (28)$$

where, $D_{H^+}$ is diffusivity of $H^+$ ion in the solution in m$^2$/s and $D^o_{H^+}$ is diffusivity of $H^+$ ion at infinite dilution and solution temperature in m$^2$/s. $D^o_{H^+}$ was obtained using the diffusivity temperature correction Eq. (14):

$$D^o_{H^+} = 9.312 \times 10^{-9} \frac{T}{298.15} \frac{\mu_{298.15,w}}{\mu_w} \exp\left[837.790\left(\frac{1}{T} - \frac{1}{298.15}\right)\right] \quad (29)$$

where, $T$ is the solution temperature in Kelvin, and $\mu_{298.15,w}$ and $\mu_w$ are the viscosity of water at 298.15 K and solution temperature ($T$). Viscosity values were determined using the Mao and Duan [65] model.

The Levich and Eisenberg equations are presented here in a somewhat unconventional format in order to explicitly elucidate the role of each of the three physical properties in the $i_{Lim}$ equations. The limiting current density $i_{Lim}$ exhibits a direct dependence on the solution density, diffusivity, and concentration of $H^+$ ions in the bulk solution and is inversely related to the solution viscosity [106,234–237]. To determine the density and viscosity of the solution, as well as the diffusivity of $H^+$ ions, we employed models recommended in this review. The concentration of $H^+$ ion was calculated using the mixed solved electrolyte (MSE) model [109,180]. A detailed discussion about the effect of NaCl concentration on $H^+$ concentration has been reported elsewhere [109, 238].

To clearly understand the influence of solution density, viscosity, and $H^+$ ion diffusivity on the variation of $i_{Lim}$ with NaCl concentration, a unique methodology was employed. Five distinct scenarios were defined, and $i_{Lim}$ was computed cumulatively for these scenarios to assess the individual contribution of each parameter to the calculated $i_{Lim}$ values. These five scenarios are outlined as follows:

- *Pure water scenario*: assuming that none of the four parameters, solution density, viscosity, $H^+$ diffusivity, and $H^+$ concentration change with NaCl concentration, and that they are the same as those for pure water.
- *Rho scenario*: assuming that only solution density changes with NaCl concentration, while solution viscosity, $H^+$ diffusivity, and $H^+$ concentration remain constant and the same as those for pure water.
- *Rho+Mu scenario*: assuming that solution density and viscosity change with NaCl concentration, while $H^+$ diffusivity and $H^+$ concentration remain constant and the same as those for pure water.
- *Rho+Mu+D scenario*: assuming that solution density, viscosity, and $H^+$ diffusivity change with NaCl concentration, while $H^+$ concentration remains constant and the same as that for pure water.
- *Rho+Mu+D+c scenario*: assuming that all four parameters, solution density, viscosity, $H^+$ diffusivity, and $H^+$ concentration change with NaCl concentration.

In the *Pure water* scenario, the impact of salt concentration on any of the parameters contributing to $i_{Lim}$ is not taken into account. Consequently, $i_{Lim}$ remains constant across all NaCl concentrations, mirroring that of pure water. As anticipated, in this scenario, the calculated $i_{Lim}$ values deviate significantly from the measured values, as presented in Fig. 8. The *Rho* and *Rho+Mu* scenarios show how changes in solution density and viscosity with NaCl concentration, respectively, contribute to the $i_{Lim}$ variations. Notably, the changes in the solution density alone when NaCl concentration is increased from 0 to 20 wt.% has almost no effect on $i_{Lim}$. When the variations in the solution viscosity with increasing NaCl concentration within the same range are included in the calculations, a larger influence on $i_{Lim}$ can be seen compared to that imposed by the solution density, yet still relatively small. The *Rho+Mu+D* scenario highlights the effect of $H^+$ diffusivity variations with varying NaCl concentration on $i_{Lim}$. From Fig. 8, it is obvious that changes in $H^+$ diffusivity exert a more pronounced impact on $i_{Lim}$ compared to the variations in the other two parameters. Ultimately, when the effect of salt concentration on $H^+$ concentration is added to the $i_{Lim}$ calculations in the *Rho+Mu+D+c* scenario, the final $i_{Lim}$ line (the solid black line in Fig. 8) is obtained.

The comparison between the calculated $i_{Lim}$ values (solid black lines) and the experimental values in Fig. 8 shows a high degree of agreement between these values. This alignment indicates that the models used in this study for the estimation of solution density and viscosity, $H^+$ diffusivity, and $H^+$ concentration are reasonably accurate. Furthermore, the overall decreasing trend observed in $i_{Lim}$ with increasing NaCl concentration can be primarily attributed to the decrease in $H^+$ diffusivity and $H^+$ ion bulk concentration, stemming from the non-ideality of the solution. A peak can be seen at low NaCl concentrations in the calculated $i_{Lim}$ values which is because of the trend in $H^+$ ion bulk concentration with varying NaCl concentration [109,238].

However, it is worth noting that this peak was not detected in the experimental $i_{Lim}$ data, likely due to the insufficient resolution in the experimental NaCl concentrations. Conducting electrochemical $i_{Lim}$ measurements in solutions with very low salt concentrations is rather difficult, owing to the low conductivity of the aqueous solution, which results in significant interference with current density readings and increase experimental errors. This type of peak was observed in similar experiments in $CO_2$ saturated solutions, as reported by Madani Sani *et al* [237,238]. In those experiments, the solution conductivity at low salt concentrations was higher due to the presence of dissolved carbonic species and did not significantly affect the $i_{Lim}$ measurements. Furthermore, the $CO_2$ corrosion rate, controlled by the cathodic limiting current density, showed a similar peak at very low NaCl concentrations.

In summary, the analysis presented above highlights the importance of accurate models for calculating all four physical properties: solution density and viscosity, $H^+$ diffusivity, and $H^+$ ion concentration as a function of salt concentration. However, it becomes evident that achieving precision in the calculations for $H^+$ diffusivity and $H^+$ ion concentration is more critical than for solution density and viscosity when calculating mass transfer rates for $i_{Lim}$.

## 7. Conclusions

This work provides a review and comparison of publicly available and well-cited models for density, viscosity, and diffusivity in aqueous NaCl solutions. Numerous models have been published for these three parameters; however, their accuracy has not been evaluated, particularly close to the limits of their validity range, using experimental data

from various sources. In this study five density models, three viscosity models, and five diffusivity models were reviewed to identify the most accurate yet simple-to-replicate ones. Additionally, one of the existing models for the effect of dissolved $CO_2$ concentration on viscosity of aqueous NaCl solutions has been modified. Furthermore, the diffusivity of multiple species at 25°C and infinite dilution in water is revisited. To estimate diffusivity at various temperatures and salt concentrations, new coefficients are introduced for selected species. These models were combined to calculate the electrochemical cathodic limiting current density ($i_{Lim}$), an important parameter with applications in various research and industrial fields. The calculated $i_{Lim}$ values have been found to agree well with those measured in this study using two-electrode setups over a wide range of NaCl concentrations. The $i_{Lim}$ analysis indicated that obtaining accurate calculations for diffusivity is more critical than solution density and viscosity when calculating mass transfer rates of dissolved species in aqueous solutions.

## CRediT authorship contribution statement

**Fazlollah Madani Sani:** Conceptualization, Data curation, Formal analysis, Methodology, Validation, Visualization, Writing – original draft, Writing – review & editing. **Srdjan Nesic:** Conceptualization, Formal analysis, Project administration, Supervision, Validation, Writing – review & editing.

## Declaration of competing interest

The authors declare that they have no known competing financial interests or personal relationships that could have appeared to influence the work reported in this paper.

## Data availability

Data will be made available on request.

## References


[1] D.B. Burnett, Potential for Beneficial Use of Oil and Gas Produced Water, Global Petroleum Institute, Texas Water Resources Institute, Texas A&M University, 2004.

[2] K. Lee, J. Neff (Eds.), Produced Water: Environmental Risks and Advances in Mitigation Technologies, First Edition, Springer, New York, NY, 2011, https://doi.org/10.1007/978-1-4614-0046-2.

[3] M. Reed, S. Johnsen, Produced Water 2: Environmental Issues and Mitigation Technologies, Plenum Press, New York, NY, 2012.

[4] E.T. Igunnu, G.Z. Chen, Produced water treatment technologies, Int. J. Low-Carbon Technol. 9 (2014) 157–177, https://doi.org/10.1093/ijlct/cts049.

[5] G. Neupane, D. Wendt, Assessment of mineral resources in geothermal brines in the US, in: 42nd Workshop Geotherm. Reserv. Eng, Stanford University, Stanford University, Stanford, CA, 2017. Paper No. SGP-TR-212.

[6] S.L. Phillips, A.K. Mathur, G. Warren, Treatment of geothermal brines. Geotherm. Scaling Corros, First Edition, American Society for Testing and Materials, Baltimore, MD, 1980, pp. 207–224.

[7] P. Loganathan, G. Naidu, S. Vigneswaran, Mining valuable minerals from seawater: a critical review, Environ. Sci. Water Res. Technol. 3 (2017) 37–53, https://doi.org/10.1039/C6EW00268D.

[8] M.L. Vera, W.R. Torres, C.I. Galli, A. Chagnes, V. Flexer, Environmental impact of direct lithium extraction from brines, Nat. Rev. Earth Environ. 4 (2023) 149–165, https://doi.org/10.1038/s43017-022-00387-5.

[9] T.F. O'Brien, T.V. Bommaraju, F. Hine, Handbook of Chlor-Alkali Technology: Volume I: Fundamentals, Volume II: Brine Treatment and Cell Operation, Volume III: Facility Design and Product Handling, Volume IV: Operations, Volume V: Corrosion, Environmental Issues, and Future Developments, Springer Science & Business Media, 2007.

[10] P.E. Muehlberg, B.P. Shepherd, J.T. Redding, H.C. Behrens, T. Parsons, Industrial Process Profiles for Environmental Use, Chapter 15: Brine and Evaporite Chemicals Industry, Industrial Environmental Research Laboratory, Cincinnati, OH, 1977.

[11] A. Panagopoulos, K.-J. Haralambous, Environmental impacts of desalination and brine treatment - challenges and mitigation measures, Mar. Pollut. Bull. 161 (2020) 111773, https://doi.org/10.1016/j.marpolbul.2020.111773.

[12] S.A. Abdul-Wahab, M.A. Al-Weshahi, Brine management: substituting chlorine with on-site produced sodium hypochlorite for environmentally improved desalination processes, Water Resour. Manag. 23 (2009) 2437–2454, https://doi.org/10.1007/s11269-008-9389-7.

[13] M.D. Holloway, C. Nwaoha, O.A. Onyewuenyi, Process Plant Equipment: Operation, Control, and Reliability, First Edition, John Wiley & Sons, Germany, 2012.

[14] H.T. Vulté, Food Industries: An Elementary Text-book on the Production and Manufacture of Staple Foods, Designed for Use in High Schools and Colleges, First Edition, The Chemical Publishing Company, Easton, PA, 1914.

[15] G. Caldwell, Mastering Basic Cheesemaking: The Fun and Fundamentals of Making Cheese at Home, First Edition, New Society Publishers, Gabriola Island, Canada, 2016.

[16] C.E. Clark, J.A. Veil, Produced Water Volumes and Management Practices in the United States, U.S. Department of Energy, Office of Fossil Energy, National Energy Technology Laboratory, Argonne National Laboratory, 2009.

[17] G.N. Breit, USGS Produced Waters Database, U.S. Department of the Interior, 2002.

[18] J. Veil, U.S. Produced Water Volumes and Management Practices in 2012, Veil Environmental, LLC, 2015.

[19] M. Meehan, T. DeSutter, K. Sedivec, C. Augustin, A. Peterson, Environmental Impacts of Brine (Produced Water), North Dakota State University, 2023.

[20] E. Allison, B. Mandler, Water in the Oil and Gas Industry: An Overview of the Many Roles of Water in Oil and Gas Operations, American Geosciences Institute, 2018.

[21] M. Mburu, Feasibility study on direct utilisation of energy from geothermal brine – a case study of Olkaria geothermal power plant, Kenya. World Geotherm. Congr, International Geothermal Association, Bali, Indonesia, 2010.

[22] A. Lopez, B. Roberts, D. Heimiller, N. Blair, G. Porro, U.S. renewable energy technical potentials. A GIS-based analysis, 2012, https://doi.org/10.2172/1219777.

[23] The Geysers and Salton Sea Geothermal Fields, California State Lands Commission, 2015.

[24] J.P. Carter, F.X. McCawley, S.D. Cramer, J. Needham, Corrosion Studies in Brines of the Salton Sea Geothermal Field, Avondale Metallurgy Research Center; Bureau of Mines, Washington, DCUSA, 1979, https://doi.org/10.2172/6305325. Avondale, Md.

[25] F.X. McCawley, S.D. Cramer, W.D. Riley, J.P. Carter, J. Needham, Corrosion of Materials and Scaling in Low-Salinity East Mesa Geothermal Brines, Bureau of Mines, United States Department of The Interior, 1981, https://doi.org/10.2172/6883071.

[26] M. Nordsveen, S. Nešić, R. Nyborg, A. Stangeland, A mechanistic model for carbon dioxide corrosion of mild steel in the presence of protective iron carbonate films—Part 1: theory and verification, Corrosion 59 (2003) 443–456, https://doi.org/10.5006/1.3277576.

[27] S. Nesic, Y. Zheng, N. Jing, S. Navabzadeh Esmaeely, Z. Ma, FREECORPTM 2.0 Theoretical Background and Verification, Institute for Corrosion and Multiphase Technology, Ohio University, Athens, OH, 2018. https://www.icmt.ohio.edu/web/software/public/release/FREECORPTM.pdf.

[28] A. Kahyarian, S. Nesic, A new narrative for $CO_2$ corrosion of mild steel, J. Electrochem. Soc. 166 (2019) C3048–C3063, https://doi.org/10.1149/2.0071911jes.

[29] P.S. Abdar, M.B. Hariri, A. Kahyarian, S. Nesic, A revision of mechanistic modeling of mild steel corrosion in $H_2S$ environments, Electrochimica Acta 382 (2021) 138231, https://doi.org/10.1016/j.electacta.2021.138231.

[30] A. Kahyarian, A. Schumaker, B. Brown, S. Nesic, Acidic corrosion of mild steel in the presence of acetic acid: mechanism and prediction, Electrochimica Acta 258 (2017) 639–652, https://doi.org/10.1016/j.electacta.2017.11.109.

[31] Y. Zheng, J. Ning, B. Brown, S. Nešić, Electrochemical model of mild steel corrosion in a mixed $H_2S/CO_2$ aqueous environment in the absence of protective corrosion product layers, Corrosion 71 (2015) 316–325, https://doi.org/10.5006/1287.

[32] W.D. MacDonald, J.S. Grauman, Exposure testing of UNS R53400, R56404 and N06625 in Simulated Salton Sea Geothermal Brine, NACE International, Phoenix, AZ, 2018, p. 11547.

[33] M.A. McKibben, A.E. Williams, S. Okubo, Metamorphosed Plio-Pleistocene evaporites and the origins of hypersaline brines in the Salton Sea geothermal system, California: fluid inclusion evidence, Geochim. Cosmochim. Acta. 52 (1988) 1047–1056, https://doi.org/10.1016/0016-7037(88)90259-1.

[34] D.A. Anati, The salinity of hypersaline brines: concepts and misconceptions, Int. J. Salt Lake Res. 8 (1999) 55–70, https://doi.org/10.1007/BF02442137.

[35] K. Guerra, K. Dahm, S. Dundorf, Reclamation Managing Water in the West: Oil and Gas Produced Water Management and Beneficial Use in the Western United States, US Department of the Interior Bureau of Reclamation, 2011.

[36] K.S. Pitzer, J.C. Peiper, R.H. Busey, Thermodynamic properties of aqueous sodium chloride solutions, J. Phys. Chem. Ref. Data. 13 (1984) 1–102, https://doi.org/10.1063/1.555709.

[37] J. Nelson, Distribution of brine wells in the Conterminous United States, 2015.

[38] Selective Recovery of Lithium from Geothermal Brines: Final Project Report, California Energy Commission, Sacramento, Calif, 2020.

[39] M.S. Blondes, K.D. Gans, M.A. Engle, Y.K. Kharaka, M.E. Reidy, V. Saraswathula, J.J. Thordsen, E.L. Rowan, E.A. Morrissey, U.S. geological survey national produced waters geochemical database v2.3, 2019, https://doi.org/10.5066/F7J964W8.

[40] J.O. Bockris, A.K.N. Reddy, Modern Electrochemistry: An Introduction to an Interdisciplinary Area, A Plenum/Rosetta, Plenum Publishing Corporation, 1973, https://doi.org/10.1007/978-1-4615-8600-5.

[41] M. Batzle, Z. Wang, Seismic properties of pore fluids, Geophysics 57 (1992) 1396–1408, https://doi.org/10.1190/1.1443207.

[42] A.M.Jr. Rowe, J.C.S. Chou, Pressure-volume-temperature-concentration relation of aqueous sodium chloride solutions, J. Chem. Eng. Data. 15 (1970) 61–66, https://doi.org/10.1021/je60044a016.

[43] P.S.Z. Rogers, K.S. Pitzer, Volumetric properties of aqueous sodium chloride solutions, J. Phys. Chem. Ref. Data. 11 (1982) 15–81, https://doi.org/10.1063/1.555660.

[44] J.L. Haas, An equation for the density of vapor-saturated NaCl-$H_2O$ solutions from 75 degrees to 325 degrees C, Am. J. Sci. 269 (1970) 489–493, https://doi.org/10.2475/ajs.269.5.489.

[45] O. Sohnel, P. Novotny, Densities of Aqueous Solutions of Inorganic Substances, Elsevier, 1985.

[46] P. Novotny, O. Sohnel, Densities of binary aqueous solutions of 306 inorganic substances, J. Chem. Eng. Data. 33 (1988) 49–55, https://doi.org/10.1021/je00051a018.

[47] J.A. Gates, R.H. Wood, Densities of aqueous solutions of sodium chloride, magnesium chloride, potassium chloride, sodium bromide, lithium chloride, and calcium chloride from 0.05 to 5.0 mol $kg^{-1}$ and 0.1013 to 40 MPa at 298.15 K, J. Chem. Eng. Data. 30 (1985) 44–49, https://doi.org/10.1021/je00039a015.

[48] J.C. Tanger, K.S. Pitzer, Thermodynamics of NaCl-$H_2O$: a new equation of state for the near-critical region and comparisons with other equations for adjoining regions, Geochim. Cosmochim. Acta. 53 (1989) 973–987, https://doi.org/10.1016/0016-7037(89)90203-2.

[49] S.N. Lvov, R.H. Wood, Equation of state of aqueous NaCl solutions over a wide range of temperatures, pressures and concentrations, Fluid Phase Equilibria 60 (1990) 273–287, https://doi.org/10.1016/0378-3812(90)85057-H.

[50] E.J. Lam, M.N. Alvarez, M.E. Galvez, E.B. Alvarez, A model for calculating the density of aqueous multicomponent electrolyte solutions, J. Chil. Chem. Soc. 53 (2008) 1393–1398, https://doi.org/10.4067/S0717-97072008000100015.

[51] T. Driesner, The system $H_2O$–NaCl. Part II: correlations for molar volume, enthalpy, and isobaric heat capacity from 0 to 1000°C, 1 to 5000bar, and 0 to 1 $X_{NaCl}$, Geochim. Cosmochim. Acta. 71 (2007) 4902–4919, https://doi.org/10.1016/j.gca.2007.05.026.

[52] S. Mao, Z. Duan, The P, V,T,x properties of binary aqueous chloride solutions up to T=573K and 100MPa, J. Chem. Thermodyn. 40 (2008) 1046–1063, https://doi.org/10.1016/j.jct.2008.03.005.

[53] H.C. Helgeson, D.H. Kirkham, Theoretical prediction of the thermodynamic behavior of aqueous electrolytes at high pressures and temperatures; I, Summary of the thermodynamic/electrostatic properties of the solvent, Am. J. Sci. 274 (1974) 1089–1198, https://doi.org/10.2475/ajs.274.10.1089.

[54] L. Haar, E.A. Haar, J.S. Gallagher, G.S. Kell, NBS/NRC Steam Tables: Thermodynamic and Transport Properties and Computer Programs for Vapor and Liquid States of Water in SI Units, Hemisphere Publishing Corporation, 1984.

[55] F.E. Jones, G.L. Harris, ITS-90 Density of Water Formulation for Volumetric Standards Calibration, J. Res. Natl. Inst. Stand. Technol. 97 (1992) 335–340, https://doi.org/10.6028/jres.097.013.

[56] W. Wagner, A. Pruss, The IAPWS formulation 1995 for the thermodynamic properties of ordinary water substance for general and scientific use, J. Phys. Chem. Ref. Data. 31 (2002) 387–535, https://doi.org/10.1063/1.1461829.

[57] W. Wagner, J.R. Cooper, A. Dittmann, J. Kijima, H.J. Kretzschmar, A. Kruse, R. Mares, K. Oguchi, H. Sato, I. Stocker, O. Sifner, Y. Takaishi, I. Tanishita, J. Trubenbach, Th. Willkommen, The IAPWS industrial formulation 1997 for the thermodynamic properties of water and steam, J. Eng. Gas Turbines Power. 122 (2000) 150–184, https://doi.org/10.1115/1.483186.

[58] J. Hu, Z. Duan, C. Zhu, I.-M. Chou, PVTx properties of the $CO_2$–$H_2O$ and $CO_2$–$H_2O$–NaCl systems below 647 K: assessment of experimental data and thermodynamic models, Chem. Geol. 238 (2007) 249–267, https://doi.org/10.1016/j.chemgeo.2006.11.011.

[59] R.W. Potter, D.L. Brown, The Volumetric Properties of Aqueous Sodium Chloride Solutions from 0 Degrees to 500 Degrees C at Pressures up to 2000 Bars based on a Regression of the Available Literature Data, U.S. Geological Survey, 1975, https://doi.org/10.3133/ofr75636.

[60] H.J. Albert, R.H. Wood, High-precision flow densimeter for fluids at temperatures to 700 K and pressures to 40 MPa, Rev. Sci. Instrum. 55 (1984) 589–593, https://doi.org/10.1063/1.1137775.

[61] R.H. Perry, D.W. Green, Perry's Chemical Engineers' Handbook, McGraw-Hill, 1999.

[62] A.J. Ellis, Partial molal volumes of alkali chlorides in aqueous solution to 200°, J. Chem. Soc. Inorg. Phys. Theor. (1966) 1579–1584, https://doi.org/10.1039/J19660001579.

[63] P.S.Z. Rogers, D.J. Bradley, K.S. Pitzer, Densities of aqueous sodium chloride solutions from 75 to 200.degree.C at 20 bar, J. Chem. Eng. Data. 27 (1982) 47–50, https://doi.org/10.1021/je00027a014.

[64] S. Manohar, D. Puchalska, G. Atkinson, Pressure-volume-temperature properties of aqueous mixed electrolyte solutions: sodium chloride + barium chloride from 25 to 140.degree.C, J. Chem. Eng. Data. 39 (1994) 150–154, https://doi.org/10.1021/je00013a042.

[65] S. Mao, Z. Duan, The viscosity of aqueous alkali-chloride solutions up to 623 K, 1,000 bar, and high ionic strength, Int. J. Thermophys. 30 (2009) 1510–1523, https://doi.org/10.1007/s10765-009-0646-7.

[66] L. Korson, W. Drost-Hansen, F.J. Millero, Viscosity of water at various temperatures, J. Phys. Chem. 73 (1969) 34–39, https://doi.org/10.1021/j100721a006.

[67] J. Kestin, H.E. Khalifa, H. Sookiazian, W.A. Wakeham, Experimental investigation of the effect of pressure on the viscosity of water in the temperature range 10–150°C, Berichte Bunsenges. Für Phys. Chem. 82 (1978) 180–188, https://doi.org/10.1002/bbpc.197800008.

[68] R.C. Hendricks, R.B. McClintock, G.J. Silvestri, Revised international representations for the viscosity of water and steam and new representations for the surface tension of water, J. Eng. Power. 99 (1977) 664–678, https://doi.org/10.1115/1.3446565.

[69] A. Nagashima, Viscosity of water substance—new international formulation and its background, J. Phys. Chem. Ref. Data. 6 (1977) 1133–1166, https://doi.org/10.1063/1.555562.

[70] J.V. Sengers, J.T.R. Watson, Improved international formulations for the viscosity and thermal conductivity of water substance, J. Phys. Chem. Ref. Data. 15 (1986) 1291–1314, https://doi.org/10.1063/1.555763.

[71] M.L. Huber, R.A. Perkins, A. Laesecke, D.G. Friend, J.V. Sengers, M.J. Assael, I. N. Metaxa, E. Vogel, R. Mareš, K. Miyagawa, New International formulation for the viscosity of $H_2O$, J. Phys. Chem. Ref. Data. 38 (2009) 101–125, https://doi.org/10.1063/1.3088050.

[72] J.L.M. Poiseuille, Ann. Chim. Phys. 21 (1847) 76.

[73] M.P. Applebey, The viscosity of salt solutions, R. Soc. Chem. (1910) 2000–2025.

[74] G. Jones, M. Dole, The viscosity of aqueous solutions of strong electrolytes with special reference to barium chloride, J. Am. Chem. Soc. 51 (1929) 2950–2964, https://doi.org/10.1021/ja01385a012.

[75] J.D. Bernal, R.H. Fowler, A theory of water and ionic solution, with particular reference to hydrogen and hydroxyl Ions, J. Chem. Phys. 1 (1933) 515, https://doi.org/10.1063/1.1749327.

[76] K.D. Collins, Charge density-dependent strength of hydration and biological structure, Biophys. J. 72 (1997) 65–76, https://doi.org/10.1016/S0006-3495(97)78647-8.

[77] G. Jones, M. Dole, The viscosity of aqueous solutions of strong electrolytes with special reference to barium chloride, J. Am. Chem. Soc. 51 (1929) 2950–2964, https://doi.org/10.1021/ja01385a012.

[78] T. Nakai, S. Sawamura, Y. Taniguchi, Effect of pressure on the viscosity of aqueous cesium chloride solution at 25°C, J. Mol. Liq. 65–66 (1995) 365–368, https://doi.org/10.1016/0167-7322(95)00832-4.

[79] M. Afzal, M. Saleem, M.T. Mahmood, Temperature and concentration dependence of viscosity of aqueous electrolytes from 20.degree.C to 50.degree.C chlorides of (sodium(1+), potassium(1+), magnesium(2+), calcium(2+), barium(2+), strontium(2+), cobalt(2+), nickel(2+), copper(2+) and chromium(3+), J. Chem. Eng. Data 34 (1989) 339–346, https://doi.org/10.1021/je00057a023.

[80] V.M.M. Lobo, V.M.M. Quaresma, Handbook of Electrolyte Solutions, Parts A and B, Elsevier Science, 1989.

[81] H.T. Kwak, G. Zhang, S. Chen, The Effects of Salt Type and Salinity On Formation Water Viscosity and NMR Responses, Int. Symp. Soc. Core Anal., Toronto, Ca, 2005. SCA2005-51.

[82] H. Falkenhagen, M. Dole, The internal friction of electrolytic solutions and its interpretation according to debye theory, Z. Phys. 30 (1929) 611–616.

[83] H. Falkenhagen, E.L. Vernon, The viscosity of strong electrolyte solutions according to electrostatic theory, Lond. Edinb. Dublin Philos. Mag. J. Sci. 14 (1932) 537–565, https://doi.org/10.1080/14786443209462095.

[84] H. Ozbek, J.A. Fair, S.L. Phillips, Viscosity of Aqueous Sodium Chloride Solutions from 0-150°C, Energy and Environment Division, Lawrence Brekeley Laboratory, University of California, Brekeley, Ca, 1977.

[85] H.L. Zhang, S.J. Han, Viscosity and density of water + sodium chloride + potassium chloride solutions at 298.15 K, J. Chem. Eng. Data. 41 (1996) 516–520, https://doi.org/10.1021/je9501402.

[86] M. Kaminsky, The concentration and temperature dependence of the viscosity of aqueous solutions of strong electrolytes. III. KCl, $K_2SO_4$, $MgCl_2$, $BeSO_4$, and $MgSO_4$ solutions, Z. Phys. Chem. (1957) 206–231.

[87] A.A. Aleksandrov, E.V. Dzhuraeva, V.F. Utenkov, Viscosity of aqueous solutions of sodium chloride, High Temp 50 (2012) 354–358, https://doi.org/10.1134/S0018151X12030029.

[88] R.I. Pepinov, V.D. Yusufova, N.V. Lobkova, Thermodynamics of the viscous flow of aqueous solutions of sodium chloride, Russ. J. Phys. Chem. 53 (1979) 172–173.

[89] J. Kestin, H.E. Khalifa, Y. Abe, C.E. Grimes, H. Sookiazian, W.A. Wakeham, Effect of pressure on the viscosity of aqueous sodium chloride solutions in the temperature range 20-150.degree.C, J. Chem. Eng. Data. 23 (1978) 328–336, https://doi.org/10.1021/je60079a011.

[90] J. Kestin, H.E. Khalifa, R.J. Correia, Tables of the dynamic and kinematic viscosity of aqueous NaCl solutions in the temperature range 20–150 °C and the pressure range 0.1–35 MPa, J. Phys. Chem. Ref. Data. 10 (1981) 71–88, https://doi.org/10.1063/1.555641.

[91] J.P. Spivey, W.D.Jr. McCain, R. North, Estimating density, formation volume factor, compressibility, methane solubility, and viscosity for oilfield brines at temperatures from 0 to 275°C, pressures to 200 MPa, and salinities to 5.7 mole/kg, J. Can. Pet. Technol. 43 (2004), https://doi.org/10.2118/04-07-05.

[92] A.W. Islam, E.S. Carlson, Viscosity models and effects of dissolved $CO_2$, Energy Fuels 26 (2012) 5330–5336, https://doi.org/10.1021/ef3006228.

[93] C.E. Ruby, J. Kawai, The densities, equivalent conductances and relative viscosities at 25°, of solutions of hydrochloric acid, potassium chloride and sodium chloride, and of their binary and ternary mixtures of constant chloride-ion-constituent content, J. Am. Chem. Soc. 48 (1926) 1119–1128, https://doi.org/10.1021/ja01416a001.

[94] D.E. Goldsack, A.A. Franchetto, The viscosity of concentrated electrolyte solutions—III. A mixture law, Electrochimica Acta 22 (1977) 1287–1294, https://doi.org/10.1016/0013-4686(77)87012-6.

[95] S.L. Phillips, H. Ozbek, A. Igbene, G. Litton, Viscosity of NaCl and Other Solutions up to 350°C and 50 MPa Pressures, Lawrence Berkeley Laboratory, University of California, Berkeley, CA, 1980.
[96] D.J.P. Out, J.M. Los, Viscosity of aqueous solutions of univalent electrolytes from 5 to 95°C, J. Solut. Chem. 9 (1980) 19–35, https://doi.org/10.1007/BF00650134.
[97] A. Anderko, Modeling of Aqueous Corrosion. Shreirs Corros, Elsevier, 2010, pp. 1585–1629, https://doi.org/10.1016/B978-044452787-5.00083-4.
[98] Y. Zheng, Electrochemical Mechanism and Model of $H_2S$ Corrosion of Carbon Steel, PhD, Ohio University, 2015.
[99] A. Kahyarian, B. Brown, S. Nesic, The unified mechanism of corrosion in aqueous weak acids solutions: a review of the recent developments in mechanistic understandings of mild steel corrosion in the presence of carboxylic acids, carbon dioxide, and hydrogen sulfide, Corrosion 76 (2020) 268–278, https://doi.org/10.5006/3474.
[100] A. Kahyarian, M. Singer, S. Nesic, Modeling of uniform $CO_2$ corrosion of mild steel in gas transportation systems: a review, J. Nat. Gas Sci. Eng. 29 (2016) 530–549, https://doi.org/10.1016/j.jngse.2015.12.052.
[101] W. Yan, Y. Xiang, W. Li, J. Deng, Downhole $CO_2$ partial pressure calculation and tubing material selection – a case study of an offshore oil field in the South China Sea, Anti-Corros, Methods Mater 63 (2016) 414–420, https://doi.org/10.1108/ACMM-04-2016-1662.
[102] Z.M. Wang, G.-L. Song, J. Zhang, Corrosion control in $CO_2$ enhanced oil recovery from a perspective of multiphase fluids, Front. Mater. 6 (2019), https://doi.org/10.3389/fmats.2019.00272.
[103] S. Bando, F. Takemura, M. Nishio, E. Hihara, M. Akai, Viscosity of aqueous NaCl solutions with dissolved $CO_2$ at (30 to 60)°C and (10 to 20) MPa, J. Chem. Eng. Data. 49 (2004) 1328–1332, https://doi.org/10.1021/je049940f.
[104] M. Fleury, H. Deschamps, Electrical conductivity and viscosity of aqueous NaCl solutions with dissolved $CO_2$, J. Chem. Eng. Data. 53 (2008) 2505–2509, https://doi.org/10.1021/je8002628.
[105] F.Madani Sani, The main role of salt in uniform $CO_2$ corrosion: updates in modeling non-ideal water chemistry, in: CC JIP Advisory Board Meeting, Athens, Ohio, 2019.
[106] F. Madani Sani, B. Brown, S. Nesic, A Mechanistic Study on the EFFECt of Salt Concentration on Uniform Corrosion Rate of Pipeline Steel in Acidic Aqueous Environments, AMPP, Virtual, 2021, p. 16788.
[107] S.A. Rice, Comprehensive Chemical Kinetics: Diffusion-Limited Reactions, First Edition, Elsevier, New York, NY, 1985.
[108] J. Newman, K.E. Thomas-Alyea, Electrochemical Systems, Third Edition, Wiley-Interscience, Hoboken, N.J, 2004.
[109] F.Madani Sani, PhD dissertation, Ohio University, 2021.
[110] D.G. Miller, Estimation of Tracer Diffusion Coefficients of Ions in Aqueous Solution, Lawrence Livermore Laboratory, University of California, 1982.
[111] N.G. Pinto, E.E. Graham, Multicomponent diffusion in concentrated electrolyte solutions: effect of solvation, AIChE J 33 (1987) 436–443, https://doi.org/10.1002/aic.690330309.
[112] W.J. Thomas, I.A. Furzer, Diffusion measurements in liquids by the Gouy method, Chem. Eng. Sci. 17 (1962) 115–120, https://doi.org/10.1016/0009-2509(62)80023-2.
[113] E.L. Cussler, Diffusion: Mass Transfer in Fluid Systems, 3rd ed., Cambridge University Press, New York, NY, 2009.
[114] L.A. Woolf, Tracer diffusion of hydrogen ion in aqueous alkali chloride solutions at 25°, J. Phys. Chem. 64 (1960) 481–484, https://doi.org/10.1021/j100833a027.
[115] K. Kigoshi, T. Hashitani, The self-diffusion coefficients of carbon dioxide, hydrogen carbonate ions and carbonate ions in aqueous solutions, Bull. Chem. Soc. Jpn. 36 (1963) 1372, https://doi.org/10.1246/bcsj.36.1372. –1372.
[116] J.E. Vivian, C.J. King, Diffusivities of slightly soluble gases in water, AIChE J 10 (1964) 220–221, https://doi.org/10.1002/aic.690100217.
[117] G.W. Hung, R.H. Dinius, Diffusivity of oxygen in electrolyte solutions, J. Chem. Eng. Data. 17 (1972) 449–451, https://doi.org/10.1021/je60055a001.
[118] H. Hikita, S. Asai, H. Ishikawa, M. Seko, H. Kitajima, Diffusivities of carbon dioxide in aqueous mixed electrolyte solutions, Chem. Eng. J. 17 (1979) 77–80, https://doi.org/10.1016/0300-9467(79)80008-8.
[119] B. Jahne, G. Heinz, W. Dietrich, Measurement of the diffusion coefficients of sparingly soluble gases in water, J. Geophys. Res. Oceans. 92 (1987) 10767–10776, https://doi.org/10.1029/JC092iC10p10767.
[120] M. Khalifi, M. Zirrahi, H. Hassanzadeh, J. Abedi, Measurements of the molecular diffusion coefficient of dimethyl ether in water at T = (313.15–373.15 K) and P = (0.69–2.76 MPa), J. Chem. Eng. Data. 66 (2021) 2754–2763, https://doi.org/10.1021/acs.jced.1c00166.
[121] M. Jamnongwong, K. Loubiere, N. Dietrich, G. Hébrard, Experimental study of oxygen diffusion coefficients in clean water containing salt, glucose or surfactant: consequences on the liquid-side mass transfer coefficients, Chem. Eng. J. 165 (2010) 758–768, https://doi.org/10.1016/j.cej.2010.09.040.
[122] Y. Huang, C. Wu, Y. Chen, I.-M. Chou, L. Jiang, Measurement of diffusion coefficients of hydrogen sulfide in water and brine using in-situ Raman spectroscopy, Fluid Phase Equilibria 556 (2022) 113381, https://doi.org/10.1016/j.fluid.2022.113381.
[123] W. Zhang, S. Wu, S. Ren, L. Zhang, J. Li, The modeling and experimental studies on the diffusion coefficient of $CO_2$ in saline water, J. $CO_2$ Util. 11 (2015) 49–53, https://doi.org/10.1016/j.jcou.2014.12.009.
[124] V. Vitagliano, P.A. Lyons, Diffusion in aqueous acetic acid solutions, J. Am. Chem. Soc. 78 (1956) 4538–4542, https://doi.org/10.1021/ja01599a008.
[125] L. Binda, M. Bolado, A. D'Onofrio, V.M. Freytes, Analysis of a microfluidic device for diffusion coefficient determination of high molecular weight solutes detectable in the visible spectrum, Eur. Phys. J. E. 45 (2022) 56, https://doi.org/10.1140/epje/s10189-022-00211-4.
[126] A. Sell, H. Fadaei, M. Kim, D. Sinton, Measurement of $CO_2$ diffusivity for carbon sequestration: a microfluidic approach for reservoir-specific analysis, Environ. Sci. Technol. 47 (2013) 71–78, https://doi.org/10.1021/es303319q.
[127] J.T. Cullinane, G.T. Rochelle, Kinetics of carbon dioxide absorption into aqueous potassium carbonate and piperazine, Ind. Eng. Chem. Res. 45 (2006) 2531–2545, https://doi.org/10.1021/ie050230s.
[128] M.M. Wendel, R.L. Pigford, Kinetics of nitrogen tetroxide absorption in water, AIChE J 4 (1958) 249–256, https://doi.org/10.1002/aic.690040303.
[129] J.F. Perez, O.C. Sandall, Diffusivity measurements for gases in power law non-Newtonian, AIChE J 19 (1973) 1073–1075, https://doi.org/10.1002/aic.690190537.
[130] J.F. Davidson, E.J. Cullen, The determination of diffusion coefficients for sparingly soluble gases in liquids, Trans. Inst. Chem. Eng. 35 (1957) 51–60.
[131] C.E.J. Corriveau, R.L. Pigford, Absorption of $N_2O_3$ into Water, Lawrence Radiation Laboratory, University of California, Berkeley, CA, 1971.
[132] A. Tamimi, E.B. Rinker, O.C. Sandall, Diffusion coefficients for hydrogen sulfide, carbon dioxide, and nitrous oxide in water over the temperature range 293-368 K, J. Chem. Eng. Data. 39 (1994) 330–332, https://doi.org/10.1021/je00014a031.
[133] P. Raimondi, H.L. Toor, Interfacial resistance in gas absorption, AIChE J 5 (1959) 86–92, https://doi.org/10.1002/aic.690050119.
[134] H. Kramers, M.P.P. Blind, E. Snoeck, D2. Absorption of nitrogen tetroxide by water jets, Chem. Eng. Sci. 14 (1961) 115–123, https://doi.org/10.1016/0009-2509(61)85062-8.
[135] M.J. Adams, The Determination of Diffusion Coefficients of Moderately Soluble Gases in Liquids, PhD dissertation, University of London, 1963.
[136] J.L. Duda, J.S. Vrentas, Laminar liquid jet diffusion studies, AIChE J 14 (1968) 286–294, https://doi.org/10.1002/aic.690140215.
[137] I. Zandi, C.D. Turner, The absorption of oxygen by dilute polymeric solutions Molecular diffusivity measurements, Chem. Eng. Sci. 25 (1970) 517–528, https://doi.org/10.1016/0009-2509(70)80049-5.
[138] W.J. Thomas, M.J. Adams, Measurement of the diffusion coefficients of carbon dioxide and nitrous oxide in water and aqueous solutions of glycerol, Trans. Faraday Soc. 61 (1965) 668–673, https://doi.org/10.1039/TF9656100668.
[139] R.A.T.O. Nijsing, R.H. Hendriksz, H. Kramers, Absorption of $CO_2$ in jets and falling films of electrolyte solutions, with and without chemical reaction, Chem. Eng. Sci. 10 (1959) 88–104, https://doi.org/10.1016/0009-2509(59)80028-2.
[140] N. Haimour, O.C. Sandall, Molecular diffusivity of hydrogen sulfide in water, J. Chem. Eng. Data. 29 (1984) 20–22, https://doi.org/10.1021/je00035a009.
[141] F. Hershcovich, J.C. Merchuk, A. Tamir, Diffusivity of oxygen in hemoglobin solutions and red blood cell suspensions, Chem. Eng. Sci. 37 (1982) 637–641, https://doi.org/10.1016/0009-2509(82)80126-7.
[142] A. Tang, O.C. Sandall, Diffusion coefficient of chlorine in water at 25-60°C, J. Chem. Eng. Data. 30 (1985) 189–191, https://doi.org/10.1021/je00040a017.
[143] C.N. Carter, Effects of pH and Oxidizing Agents on the Rate of Absorption of Hydrogen Sulfide into Aqueous Media, PhD dissertation, Lawrence University, 1966.
[144] M.H.I. Baird, J.F. Davidson, Annular jets—II: gas absorption, Chem. Eng. Sci. 17 (1962) 473–480, https://doi.org/10.1016/0009-2509(62)85016-7.
[145] C.E. St-Denis, The Diffusion of Oxygen in Aqueous Media, PhD dissertation, UNSW Sydney, 1972, https://doi.org/10.26190/unsworks/10738.
[146] R.T. Ferrell, D.M. Himmelblau, Diffusion coefficients of hydrogen and helium in water, AIChE J 13 (1967) 702–708, https://doi.org/10.1002/aic.690130421.
[147] R.R. Walters, J.F. Graham, R.M. Moore, D.J. Anderson, Protein diffusion coefficient measurements by laminar flow analysis: method and applications, Anal. Biochem. 140 (1984) 190–195, https://doi.org/10.1016/0003-2697(84)90152-0.
[148] M.J.W. Frank, J.A.M. Kuipers, W.P.M. van Swaaij, Diffusion coefficients and viscosities of $CO_2 + H_2O$, $CO_2 + CH_3OH$, $NH_3 + H_2O$, and $NH_3 + CH_3OH$ Liquid Mixtures, J. Chem. Eng. Data. 41 (1996) 297–302, https://doi.org/10.1021/je950157k.
[149] P. Han, D.M. Bartels, Temperature dependence of oxygen diffusion in $H_2O$ and $D_2O$, J. Phys. Chem. 100 (1996) 5597–5602, https://doi.org/10.1021/jp952903y.
[150] I.M. Kolthoff, C.S. Miller, The reduction of oxygen at the dropping mercury electrode, J. Am. Chem. Soc. 63 (1941) 1013–1017, https://doi.org/10.1021/ja01849a035.
[151] J. Jordan, E. Ackerman, R.L. Berger, Polarographic diffusion coefficients of oxygen defined by activity gradients in viscous media, J. Am. Chem. Soc. 78 (1956) 2979–2983, https://doi.org/10.1021/ja01594a015.
[152] J. Jordan, W.E. Bauer, Correlations between solvent structure, viscosity and polarographic diffusion coefficients of oxygen, J. Am. Chem. Soc. 81 (1959) 3915–3919, https://doi.org/10.1021/ja01524a027.
[153] I.M. Kolthoff, K. Izutsu, The ratio of the first to the second diffusion current of oxygen at the dropping mercury electrode. Diffusion coefficient of oxygen, J. Am. Chem. Soc. 86 (1964) 1275–1279, https://doi.org/10.1021/ja01061a001.
[154] K.E. Gubbins, K.K. Bhatia, R.D. Walker, Diffusion of gases in electrolytic solutions, AIChE J 12 (1966) 548–552, https://doi.org/10.1002/aic.690120328.
[155] N.K. Roberts, H.L. Northey, Hydrogen ion mobility in aqueous electrolyte solutions. Comparison of polarographic and diaphragm cell methods, J. Chem. Soc. Faraday Trans. 1 Phys. Chem. Condens. Phases. 68 (1972) 1528–1532, https://doi.org/10.1039/F19726801528.

[156] L.-K. Ju, C.S. Ho, Measuring oxygen diffusion coefficients with polarographic oxygen electrodes: I. Electrolyte solutions, Biotechnol. Bioeng. 27 (1985) 1495–1499, https://doi.org/10.1002/bit.260271015.
[157] C.S. Ho, L.-K. Ju, R.F. Baddour, D.I.C. Wang, Simultaneous measurement of oxygen diffusion coefficients and solubilities in electrolyte solutions with a polarographic oxygen electrode, Chem. Eng. Sci. 43 (1988) 3093–3107, https://doi.org/10.1016/0009-2509(88)80061-7.
[158] S. Hirai, K. Okazaki, H. Yazawa, H. Ito, Y. Tabe, K. Hijikata, Measurement of $CO_2$ diffusion coefficient and application of LIF in pressurized water, Energy 22 (1997) 363–367, https://doi.org/10.1016/S0360-5442(96)00135-1.
[159] L. Liebermann, Air bubbles in water, J. Appl. Phys. 28 (1957) 205–211, https://doi.org/10.1063/1.1722708.
[160] G. Houghton, P.D. Ritchie, J.A. Thomson, The rate of solution of small stationary bubbles and the diffusion coefficients of gases in liquids, Chem. Eng. Sci. 17 (1962) 221–227, https://doi.org/10.1016/0009-2509(62)85001-5.
[161] D.L. Wise, G. Houghton, The diffusion coefficients of ten slightly soluble gases in water at 10–60°C, Chem. Eng. Sci. 21 (1966) 999–1010, https://doi.org/10.1016/0009-2509(66)85096-0.
[162] I.M. Krieger, G.W. Mulholland, C.S. Dickey, Diffusion coefficients for gases in liquids from the rates of solution of small gas bubbles, J. Phys. Chem. 71 (1967) 1123–1129, https://doi.org/10.1021/j100863a051.
[163] J. Irina, A spectrophotometric method for measuring diffusion coefficients, J. Chem. Educ. 57 (1980) 676, https://doi.org/10.1021/ed057p676.
[164] E.N. Dunmire, A.M. Plenys, D.F. Katz, Spectrophotometric analysis of molecular transport in gels, J. Controlled Release. 57 (1999) 127–140, https://doi.org/10.1016/S0168-3659(98)00111-4.
[165] A. Iverson, The measured resistivity of pure water and determination of the limiting mobility of OH. from 5 to 55°, J. Phys. Chem. 68 (1964) 515–521, https://doi.org/10.1021/j100785a012.
[166] B.D. Cornish, R.J. Speedy, Proton conductivity in supercooled aqueous hydrochloric acid solutions, J. Phys. Chem. 88 (1984) 1888–1892, https://doi.org/10.1021/j150653a043.
[167] A.J. van Stroe, L.J.J. Janssen, Determination of the diffusion coefficient of oxygen in sodium chloride solutions with a transient pulse technique, Anal. Chim. Acta. 279 (1993) 213–219, https://doi.org/10.1016/0003-2670(93)80320-K.
[168] R.E. Davis, G.L. Horvath, C.W. Tobias, The solubility and diffusion coefficient of oxygen in potassium hydroxide solutions, Electrochimica Acta 12 (1967) 287–297, https://doi.org/10.1016/0013-4686(67)80007-0.
[169] S.P. Cadogan, G.C. Maitland, J.P.M. Trusler, Diffusion coefficients of $CO_2$ and $N_2$ in water at temperatures between 298.15 K and 423.15 K at pressures up to 45 MPa, J. Chem. Eng. Data. 59 (2014) 519–525, https://doi.org/10.1021/je401008s.
[170] D.M. Himmelblau, Diffusion of dissolved gases in liquids, Chem. Rev. 64 (1964) 527–550, https://doi.org/10.1021/cr60231a002.
[171] M. Holz, S.R. Heil, A. Sacco, Temperature-dependent self-diffusion coefficients of water and six selected molecular liquids for calibration in accurate $^1$H NMR PFG measurements, Phys. Chem. Chem. Phys. 2 (2000) 4740–4742, https://doi.org/10.1039/B005319H.
[172] E.O. Stejskal, J.E. Tanner, Spin diffusion measurements: spin echoes in the presence of a time-dependent field gradient, J. Chem. Phys. 42 (1965) 288–292, https://doi.org/10.1063/1.1695690.
[173] G. Pages, V. Gilard, R. Martino, M. Malet-Martino, Pulsed-field gradient nuclear magnetic resonance measurements (PFG NMR) for diffusion ordered spectroscopy (DOSY) mapping, Analyst 142 (2017) 3771–3796, https://doi.org/10.1039/C7AN01031A.
[174] S.S. Mehta, A Pulsed Field-Gradient System for Nuclear Magnetic Resonance Diffusion Experiments, University of Missouri, 1989. Master's thesis.
[175] N. Rezaei-Ghaleh, Water dynamics in highly concentrated salt solutions: a multi-nuclear NMR approach, ChemistryOpen 11 (2022) e202200080, https://doi.org/10.1002/open.202200080.
[176] H.J.V. Tyrrell, K.R. Harris, Diffusion in Liquids: A Theoretical and Experimental Study, Butterworth-Heinemann, 2013.
[177] R.A. Robinson, R.H. Stokes, Electrolyte Solutions: Second Revised Edition, Courier Corporation, 2002.
[178] J. Ahl, Tracer and Interdiffusion Measurements of Some Common Salts in Aqueous Solutions and in Porous Ceramic Media, PhD dissertation, Aalto University, 2014.
[179] D. Li, Z. Duan, The speciation equilibrium coupling with phase equilibrium in the $H_2O$–$CO_2$–NaCl system from 0 to 250°C, from 0 to 1000 bar, and from 0 to 5 molality of NaCl, Chem. Geol. 244 (2007) 730–751, https://doi.org/10.1016/j.chemgeo.2007.07.023.
[180] R.D. Springer, P. Wang, A. Anderko, Modeling the properties of $H_2S/CO_2$/salt/water systems in wide ranges of temperature and pressure, SPE J. 20 (2015) 134, https://doi.org/10.2118/173902-PA, 1,120-1.
[181] R. Mills, Diffusion in electrolytes, J. Electroanal. Chem. 9 (1965) (1959) 57–69, https://doi.org/10.1016/0022-0728(65)80065-1.
[182] Z. Li, L. Yuan, G. Sun, J. Lv, Y. Zhang, Experimental determination of $CO_2$ diffusion coefficient in a brine-saturated core simulating reservoir condition, Energies 14 (2021) 540, https://doi.org/10.3390/en14030540.
[183] C.R. Wilke, P. Chang, Correlation of diffusion coefficients in dilute solutions, AIChE J 1 (1955) 264–270, https://doi.org/10.1002/aic.690010222.
[184] E.G. Scheibel, Correspondence. liquid diffusivities. vscosity of gases, Ind. Eng. Chem. 46 (1954) 2007–2008, https://doi.org/10.1021/ie50537a062.
[185] R.E. Zeebe, On the molecular diffusion coefficients of dissolved $CO_2$,$HCO_3^-$, and $CO_3^{2-}$ and their dependence on isotopic mass, Geochim. Cosmochim. Acta. 75 (2011) 2483–2498, https://doi.org/10.1016/j.gca.2011.02.010.
[186] J.W. Mutoru, A. Leahy-Dios, A. Firoozabadi, Modeling infinite dilution and Fickian diffusion coefficients of carbon dioxide in water, AIChE J 57 (2011) 1617–1627, https://doi.org/10.1002/aic.12361.
[187] A. Einstein, Über die von der molekularkinetischen Theorie der Wärme geforderte Bewegung von in ruhenden Flüssigkeiten suspendierten Teilchen, Ann. Phys. 322 (1905) 549–560, https://doi.org/10.1002/andp.19053220806.
[188] C.C. Miller, The Stokes-Einstein law for diffusion in solution, Proc. R. Soc. Lond. Ser. A. 106 (1924) 724–749, https://doi.org/10.1098/rspa.1924.0100.
[189] R. Mills, J.W. Kennedy, The self-diffusion coefficients of iodide, potassium and rubidium ions in aqueous solutions, J. Am. Chem. Soc. 75 (1953) 5696–5701, https://doi.org/10.1021/ja01118a063.
[190] G.A. Ratcliff, J.G. Holdcroft, Diffusivities of gases in aqueous electrolyte solutions, Trans. Inst. Chem. Eng. 41 (1963) 315–319.
[191] L.E. Scriven, R.L. Pigford, Fluid dynamics and diffusion calculations for laminar liquid jets, AIChE J 5 (1959) 397–402, https://doi.org/10.1002/aic.690050328.
[192] D.R. Lide, CRC Handbook of Chemistry and Physics, 84th Edition, Eighty Fourth Edition, CRC Press, 2003.
[193] Y.H. Li, S. Gregory, Diffusion of ions in sea water and in deep-sea sediments, Geochim. Cosmochim. Acta. 38 (1974) 703–714, https://doi.org/10.1016/0016-7037(74)90145-8.
[194] D.G. Leaist, P.A. Lyons, Diffusion in dilute aqueous acetic acid solutions at 25°C, J. Solut. Chem. 13 (1984) 77–85, https://doi.org/10.1007/BF00646041.
[195] W.J. Albery, A.R. Greenwood, R.F. Kibble, Diffusion coefficients of carboxylic acids, Trans. Faraday Soc. 63 (1967) 360–368, https://doi.org/10.1039/TF9676300360.
[196] M.J. Tham, R.D. Walker, K.E. Gubbins, Diffusion of oxygen and hydrogen in aqueous potassium hydroxide solutions, J. Phys. Chem. 74 (1970) 1747–1751, https://doi.org/10.1021/j100703a015.
[197] T.K. Goldstick, I. Fatt, Diffusion of oxygen in solutions of blood proteins. Chem Eng Prog Symp Ser, 1970, pp. 101–111.
[198] R.N. O'Brien, W.F. Hyslop, A laser interferometric study of the diffusion of $O_2$, $N_2$, $H_2$, and Ar into water, Can. J. Chem. 55 (1977) 1415–1421, https://doi.org/10.1139/v77-196.
[199] P.A. Witherspoon, D.N. Saraf, Diffusion of methane, ethane, propane, and n-butane in water from 25 to 43°, J. Phys. Chem. 69 (1965) 3752–3755, https://doi.org/10.1021/j100895a017.
[200] D.E. Bidstrup, C.J. Geankoplis, Aqueous molecular diffusivities of carboxylic acids, J. Chem. Eng. Data. 8 (1963) 170–173, https://doi.org/10.1021/je60017a004.
[201] G. Le Bas, The Molecular Volumes of Liquid Chemical Compounds, from the Point of View of Kopp, Longmans, Green, 1915.
[202] B.J. Krieg, S.M. Taghavi, G.L. Amidon, G.E. Amidon, In vivo predictive dissolution: transport analysis of the $CO_2$, bicarbonate in vivo buffer system, J. Pharm. Sci. 103 (2014) 3473–3490, https://doi.org/10.1002/jps.24108.
[203] S. Nesic, J. Postlethwaite, S. Olsen, An electrochemical model for prediction of corrosion of mild steel in aqueous carbon dioxide solutions, Corrosion 52 (1996) 280–294, https://doi.org/10.5006/1.3293640.
[204] M.S. Helal, H.A. Farag, M.S. Mansour, Y.O. Fouad, Experimental study of the diffusion-controlled corrosion of copper in the bottom of a jet stirred reactor, Braz. J. Chem. Eng. 35 (2018) 101–110, https://doi.org/10.1590/0104-6632.20180351s20160333.
[205] A. Anderko, M.M. Lencka, Computation of electrical conductivity of multicomponent aqueous systems in wide concentration and temperature ranges, Ind. Eng. Chem. Res. 36 (1997) 1932–1943, https://doi.org/10.1021/ie9605903.
[206] A. Anderko, M.M. Lencka, Modeling self-diffusion in multicomponent aqueous electrolyte systems in wide concentration ranges, Ind. Eng. Chem. Res. 37 (1998) 2878–2888, https://doi.org/10.1021/ie980001o.
[207] A.S. Quist, W.L. Marshall, Assignment of limiting equivalent conductances for single ions to 400°, J. Phys. Chem. 69 (1965) 2984–2987, https://doi.org/10.1021/j100893a027.
[208] R.L. Kay, J.L. Dye, The determination of the electrophoretic contribution to conductance from the concentration dependence of transference numbers, in: Proc. Natl. Acad. Sci. 49, 1963, pp. 5–11, https://doi.org/10.1073/pnas.49.1.5.
[209] P. Debye, E. Huckel, On the theory of electrolytes. I. Freezing point depression and related phenomena, Phys. Z. 24 (1923) 185–206.
[210] L. Onsager, The motion of Ions: principles and concepts, Science 166 (1969) 1359–1364, https://doi.org/10.1126/science.166.3911.1359.
[211] N.D. Pinto, E.E. Graham, Evaluation of diffusivities in electrolyte solutions using Stefan-Maxwell equations, AIChE J 32 (1986) 291–296, https://doi.org/10.1002/aic.690320216.
[212] L.J. Gosting, H.S. Harned, The application of the Onsager theory of ionic mobilities to self-diffusion, J. Am. Chem. Soc. 73 (1951) 159–161, https://doi.org/10.1021/ja01145a057.
[213] P. Wang, A. Anderko, Modeling self-diffusion in mixed-solvent electrolyte solutions, Ind. Eng. Chem. Res. 42 (2003) 3495–3504, https://doi.org/10.1021/ie030050n.
[214] M. Jardat, B. Hribar-Lee, V. Dahirel, V. Vlachy, Self-diffusion and activity coefficients of ions in charged disordered media, J. Chem. Phys. 137 (2012) 114507, https://doi.org/10.1063/1.4752111.
[215] H.J.V. Tyrrell, K.R. Harris, Chapter 8 - Diffusion in electrolytes, in: H.J.V. Tyrrell, K.R. Harris (Eds.), Diffus. Liq, Butterworth-Heinemann, 1984, pp. 387–437, https://doi.org/10.1016/B978-0-408-17591-3.50012-5.
[216] A. Kahyarian, S. Nesic, On the mechanism of carbon dioxide corrosion of mild steel: experimental investigation and mathematical modeling at elevated pressures and non-ideal solutions, Corros. Sci. 173 (2020) 108719, https://doi.org/10.1016/j.corsci.2020.108719.

[217] J. Jun, G.S. Frankel, N. Sridhar, Effect of chloride concentration and temperature on growth of 1D Pit, J. Solid State Electrochem. 19 (2015) 3439–3447, https://doi.org/10.1007/s10008-015-2780-4.
[218] R.M. Katona, J. Carpenter, E.J. Schindelholz, R.G. Kelly, Prediction of maximum pit sizes in elevated chloride concentrations and temperatures, J. Electrochem. Soc. 166 (2019) C3364, https://doi.org/10.1149/2.0451911jes.
[219] M.V. Stackelberg, M. Pilgram, Diffusionskoeffizient des wasserstoffions in wässrigen KCl-lösungen, Collect. Czechoslov. Chem. Commun. 25 (1960) 2974–2976, https://doi.org/10.1135/cccc19602974.
[220] M. Stastny, F. Strafelda, Concentration dependence of the diffusion coefficient of hydrogen ions in aqueous solutions of alkali metal salts, Collect. Czechoslov. Chem. Commun. 34 (1969) 168–176.
[221] R.H. Stokes, L.A. Woolf, R. Mills, Tracer diffusion of iodide ion in aqueous alkali chloride solutions at 25°, J. Phys. Chem. 61 (1957) 1634–1636, https://doi.org/10.1021/j150558a016.
[222] M. Ciszkowska, Z. Stojek, S.E. Morris, J.G. Osteryoung, Steady-state voltammetry of strong and weak acids with and without supporting electrolyte, Anal. Chem. 64 (1992) 2372–2377, https://doi.org/10.1021/ac00044a013.
[223] R.L. Miller, W.L. Bradford, N.E. Peters, Specific Conductance; Theoretical Considerations and Application to Analytical Quality Control, Department of the Interior, 1986, https://doi.org/10.3133/wsp2311.
[224] H.S. Harned, B.B. Owen, The Physical Chemistry of Electrolytic Solutions, Third Edition, Reinhold Pub. Corp, New York, 1958.
[225] E. Hawlicka, Self-diffusion of sodium, chloride and iodide ions in acetonitrile-water mixtures, Z. Für Naturforschung A. 42 (1987) 1014–1016, https://doi.org/10.1515/zna-1987-0915.
[226] V. Vitagliano, P.A. Lyons, Diffusion coefficients for aqueous solutions of sodium chloride and barium chloride, J. Am. Chem. Soc. 78 (1956) 1549–1552, https://doi.org/10.1021/ja01589a011.
[227] C.A.J. Appelo, Solute transport solved with the Nernst-Planck equation for concrete pores with 'free' water and a double layer, Cem. Concr. Res. 101 (2017) 102–113, https://doi.org/10.1016/j.cemconres.2017.08.030.
[228] K.A. Snyder, X. Feng, B.D. Keen, T.O. Mason, Estimating the electrical conductivity of cement paste pore solutions from $OH^-$, $K^+$ and $Na^+$ concentrations, Cem. Concr. Res. 33 (2003) 793–798, https://doi.org/10.1016/S0008-8846(02)01068-2.
[229] J. Ananthaswamy, G. Atkinson, Thermodynamics of concentrated electrolyte mixtures. 4. Pitzer-Debye-Hueckel limiting slopes for water from 0 to 100.degree. C and from 1 atm to 1 kbar, J. Chem. Eng. Data. 29 (1984) 81–87, https://doi.org/10.1021/je00035a027.
[230] D.J. Bradley, K.S. Pitzer, Thermodynamics of electrolytes. 12. Dielectric properties of water and Debye-Hueckel parameters to 350.degree.C and 1 kbar, J. Phys. Chem. 83 (1979) 1599–1603, https://doi.org/10.1021/j100475a009.
[231] C.A.J. Appelo, Specific conductance: how to calculate, to use, and the pitfalls, 2018. https://www.hydrochemistry.eu/exmpls/sc.html.
[232] T. Huang, PhD dissertation, Swinburne University of Technology, 2012.
[233] K.J. Vetter, Electrochemical Kinetics: Theoretical and Experimental Aspects, Academic Press, 1967.
[234] F. Opekar, P. Beran, Rotating disk electrodes, J. Electroanal. Chem. Interfacial Electrochem. 69 (1976) 1–105, https://doi.org/10.1016/S0022-0728(76)80129-5.
[235] B.G. Levich, Physicochemical Hydrodynamics, Prentice-Hall, Inc, 1962.
[236] M. Eisenberg, C.W. Tobias, C.R. Wilke, Ionic mass transfer and concentration polarization at rotating electrodes, J. Electrochem. Soc. 101 (1954) 306–320, https://doi.org/10.1149/1.2781252.
[237] F. Madani Sani, B. Brown, Z. Belarbi, S. Nesic, An Experimental Investigation on the Effect of Salt Concentration on Uniform $CO_2$ Corrosion, NACE International, Nashville, TN, 2019, p. 13026. Paper No.
[238] F. Madani Sani, B. Brown, S. Nesic, An electrochemical study of the effect of high salt concentration on uniform corrosion of Carbon steel in aqueous $CO_2$ solutions, J. Electrochem. Soc. 168 (2021) 051501, https://doi.org/10.1149/1945-7111/abf5f9.